Automated Non-Linear Pushover Analyses of Reinforced Concrete Structures

by

Kyle Prusinski

B. Science, Bradley University 2010

A thesis submitted to the

Faculty of the Graduate School of the

University of Colorado in partial fulfillment

of the requirements for the degree of

Master of Science

Department of Civil, Environmental and Architectural Engineering

2015

This thesis entitled:
Automated Non-Linear Pushover Analyses of Reinforced Concrete Structures
written by Kyle Prusinski
has been approved for the Department of Civil, Environmental and Architectural Engineering

Prof. Victor Saouma

Prof. Petros Sideris

Prof. Yunping Xi

Prof. Mija Hubler

Date _____

The final copy of this thesis has been examined by the signatories, and we find that both the content and the form meet acceptable presentation standards of scholarly work in the above mentioned discipline.

Prusinski, Kyle (M.S. Civil Engineering)

Automated Non-Linear Pushover Analyses of Reinforced Concrete Structures

Thesis directed by Prof. Victor Saouma

Abstract

The purpose of this thesis is to develop a guide for the means and methods entailed in a Pushover Analysis. The main components of the analysis are discussed in detail followed by the formulation of a conceptual model and computer model to carry out the design procedure from beginning to end. Furthermore, analytical results are assessed to assist engineers gain a feel for non-linear structural behavior in response to seismic events.

The study broadly covers the ductility of concrete members in a performance based engineering sense. As standard design codes implement PBE initiatives, there is a need to for the practicing engineer to have a firm understanding non-linear behavior. The analysis includes different loading as well as cross-sections that lead to the verification of the computer model, labeled ANPA, in comparison to proven methods and concepts.

Further, this design guide helps relate structural behavior of RC members when plastic hinges are introduced into the structural stiffness matrix.

The study concludes with simplified analytic verification and application of this model to satisfy drift requirements found through spectral analysis of the design earthquake.

Dedication

To my Mother, Father, and Sister for believing in my abilities and encouraging me to reach out and obtain the life goals that are most important to me.

Acknowledgements

My deepest gratitude goes to Dr. Victor Saouma for taking me on as a pupil and providing guidance over the course of the past year. It has been an honor to work with a professor so highly regarded within the development and progression of the field of Structural Engineering and Structural Mechanics.

I also want to recognize the valuable advice provided by Dr.Mija Hubler, Dr. Yunping Xi, and Dr. Petros Sideris towards improving the work. I enjoyed working with my friend and fellow student Mohammad Nikoukalam. Mohammad's counsel and advice pertaining to the Pushover concepts and final results have been instrumental to the development of this report.

Contents

Chapter

Tables

Table

Figures

Figure

Chapter 1

Introduction

1.1 Motivation

With the development of Performance Based Structural Engineering in the design world, there has been a need for designers to move away from traditional linear design methodologies in order to predict how structures will respond to loads up to and at the point of failure. This non-linear deformation measurement of the structure after its first yielding point can be defined as the ductility of the structure, and is a desirable property where resistance to brittle failure during flexure is required to ensure structural integrity. These ductile yield points are then analyzed as plastic hinges within the structure in order to model the re-distribution of stresses throughout a structure as a whole. To perform a seismic PBSE analysis, this process is continually repeated until the structure reaches a state of collapse. This kind of analysis is defined as a "Pushover" analysis and is often required during the design of structures in earthquake-prone regions. Most of these analyses are performed by non-linear software given the basic inputs such as geometry, material properties, expected load, etc. While the software analyses the complicated computations, it is up to the engineer to make sense of the results and present the findings in such a way that can be used to base decisions off of. Therefore, it is essential that we have a firm understanding of the factors that dictate the ductility of the composing members within the structure. The aim of this report is to review the theory behind the Pushover analyses of reinforced concrete structures in accordance with AASHTO Bridge Design Guidelines. A conceptual model containing the theory behind the analysis will be discussed, leading into the formation of an automated computer model to work as

an interactive design aid for the practicing structural engineer.

1.2 Thesis Outline

The report comprises the analysis of a static pushover design, arranged throughout the five following chapters. Chapter 2 focuses on the theory that supports the analysis and procedure in which a pushover analysis is to be carried out. A section is dedicated to each step of the analysis, including determining the demand displacements of a structure, the plastic properties of the members within the structure, and the different pushover methods used to define the ultimate displacement capacity of the structure of interest. The conclusion section recaps why particular means and methods are either considered more of a conservative, liberal, or somewhere in between. Chapter 3 includes the application to the means and methods of the pushover design through implementation of a MatLab defined as the Automated Non-Linear Pushover Analysis or "ANPA". Flowcharts are provided to guide the practicing engineer though the performance of the spectral analysis the moment curvature analysis and finally the structural analysis through implementation of the direct stiffness method that is the basis of how modern-day structural analysis software such as RISA ETABS and SAP2000 operates. Chapter 4 includes the verification of the principle functions within ANPA. Results from the design aid are compared to proven methods and computations currently used within the field of study by practicing professionals and University researchers. Chapter 5 implements ANPA in the analysis of a section of the proposed Goethals Bridge Replacement Project in New York. Procured data from ANPA is compared to results provided through an analysis performed by Kiewit and colleagues within the structural engineering department here at CU Boulder. Chapter 6 includes comparisons of the above mentioned structural analysis procedures and what design considerations should be taken into account in determination of whether or not the structure of interest satisfies drift requirements. Additionally, a brief description of future work that can be done to further develop this report is provided.

Chapter 2

Theory

2.1 Introduction

When performing a pushover analysis many design factors need to be considered. The expected accelerations and displacements of a structure from a seismic event can be designed for given the geographic location of the structure combined with the type of foundation the structure is built upon. Given the natural period of the structure, probabilistic acceleration and displacement demands can be defined. These acceleration and displacement demands can be designed for given the size and geometry of our columns in use. The formation of plastic hinges in reinforced concrete can then be designed for based on the moment-curvature relationship of the column. As plastic hinges form, the forces within the structure will be redistributed based on the revised stiffness in the structure. Two pushover methods are presented, one of which being a more in-depth analytic analysis that will underestimate the displacement capacity of a structure, and the other more simplified method that will slightly overestimate the displacement capacity of a structure. This section aims to define the theory behind the analyses involved within each step of the design process.

2.2 Spectral Analysis

The Design Response Spectra can be defined as the range of expected accelerations and displacements of a structure over a range of natural periods. The spectra is directly dependent on probability of the intensity of the ground shaking at a specific location during a seismic event. This probability is formulated through an analysis of historical data that takes into account the

magnitude of the earthquake, the soil conditions at the site, the fault type, and the distance from the epicenter. All of this information provides us as engineers with the probability of exceedance of ground accelerations over a certain time frame.

AASHTO guidelines specify that bridges shall be designed for life safety performance in that a bridge shall be able to withstand with a seismic hazard associated with an event that has a seven percent probability of exceedance within 75 years. This level of probability is associated with an earthquake that is expected to happen once every 1033 years. USGS maps that plot acceleration values associated with this level of seismic hazard are used to define the Design Response Spectrum of our structure. AASHTO goes about designing such a spectrum given the following values from these maps.

PGA	Peak Ground Acc. at the Geographic Location
S_S	Short Period Spectral Acc. Coefficient
S_1	1-Sec Period Spectral Acc. Coefficient

Table 2.1: USGS Geographic Values

The values from Table 2.1 are based upon the location of the site with respect to nearby faults and other potential site for seismic activity. When we look at the above values in combination with the site classification that our structure is located on, we obtain the following site specific vales.

F_{PGA}	Site Specific Peak Ground Acc.
S_{DS}	Site Specific Short Period Spectral Acc. Coefficient
S_{D1}	Site Specific 1-Sec Period Spectral Acc. Coefficient

Table 2.2: Site Soil Classification Values

The values from Table 2.2 are found through AASHTO Tables 3.4.2.3-1 & 3.4.2.3-2. It is at this point that we can develop the Design Response Spectrum using the Three-Point Method which can be performed using Fig. 2.1:

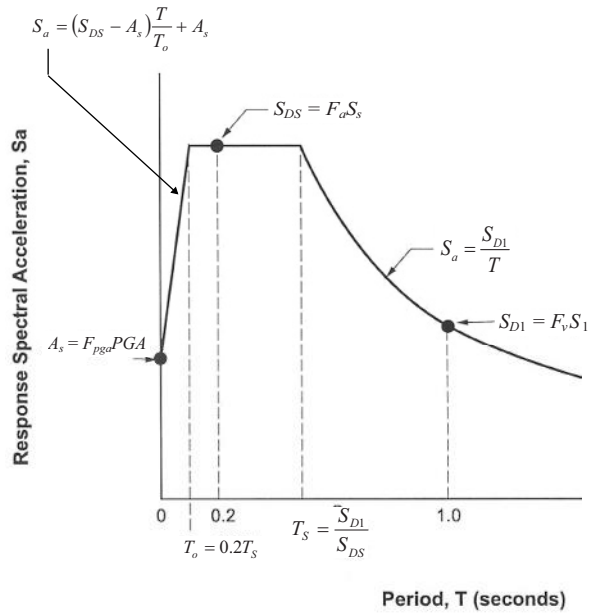

Figure 2.1: Design Spectrum

The three points A_S, S_{DS}, and S_{D1} are defined given six known acceleration from Tables 2.1 and 2.2. From these values, the spectral design curve can be found given the equations in Fig. 2.1. Knowing the spectral acceleration, the spectral displacement can be found using Equ. 2.2.

$$S_D = \left(\frac{T}{2\pi}\right)^2 * S_A * g \tag{2.1}$$

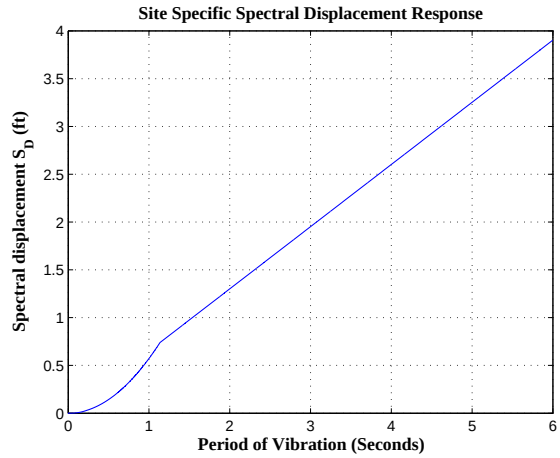

Figure 2.2: Spectral Displacement Example

The Spectral Displacement of the structure can be considered the demand displacement that our structure will have to resist through both elastic and plastic deformation. The performance-based design goal is to allow plastic deformation to occur in order to protect the entirety of the bridge from collapse during a major seismic event. In order to quantify the plastic displacement capacity of the structure, cross section properties within the structure elements first need to be analyzed.

2.3 Whitney Stress Block

The most commonly used method for determining the stresses within a concrete cross section is the Whitney Stress Block method. Concrete has a linear stress distribution up until about 45% of the material's ultimate strain. After this point, the material behaves in a non-linear fashion Park, R. and Paulay T. (1975). Fig. 2.3 shows a combination of stress-strain profiles with the strain at the most extreme fiber in compression ranging from 45% to 100% of the ultimate strain capacity of the concrete in a singly reinforced concrete beam. The figure shows that the change in location of the neutral axis and dimension of the moment arm corresponds with the change to the stress profile.

An exact measurement of the stresses within the section profile would require numerical

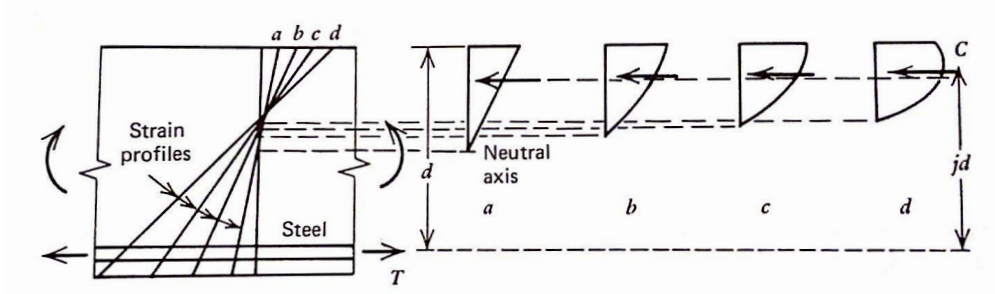

Figure 2.3: Stress as a Function of Strain in the Most Extreme Fiber

integration over the area of the section in compression. In the interest of developing a method that practicing engineers could use without having to perform this tedious analysis, Whitney developed a method of replacing the stress distribution of the confined concrete with a constant linear block as depicted in Fig. 2.4 below.

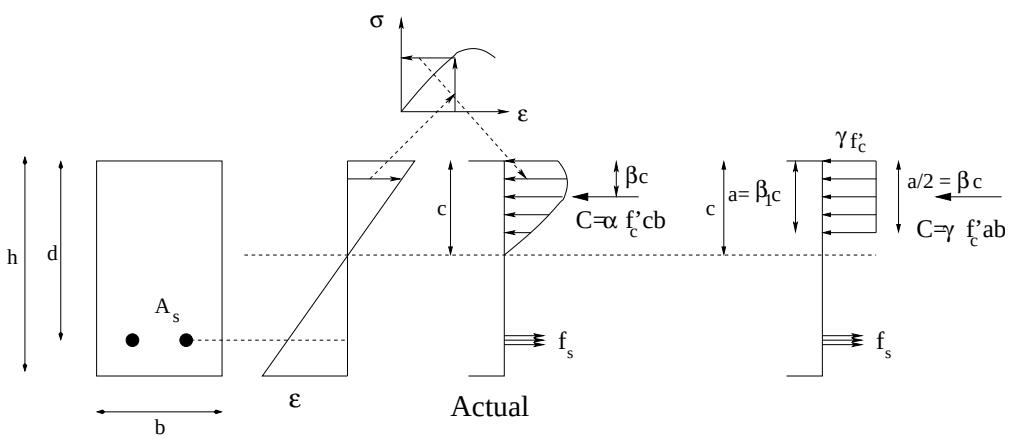

Figure 2.4: Cracked Section, Limit State

The exact stress diagram is replaced with a simpler and equivalent one, and has been adopted my most codes, (**ACI 10.2.6**) ACI (2011).

For the equivalent stress distribution, the only variables that need to be defined are C & its location, thus α and β. A rectangular stress can be defined, with depth $a = \beta_1 c$, and stress equal

to $\gamma f'_c$ **(ACI 10.2.7.1)**

$$C = \alpha f'_c bc = \gamma f'_c ab \tag{2.2}$$

$$\alpha = \frac{f_{av}}{f'_c} \tag{2.3}$$

$$a = \beta_1 c \tag{2.4}$$

Thus

$$\gamma = \frac{\alpha}{\beta_1} \tag{2.5}$$

But the location of the resultant forces must be the same, hence

$$\beta_1 = 2\beta \tag{2.6}$$

From experiments, the following coefficients in 2.3 are found

f'_c (psi)	<4,000	5,000	6,000	7,000	8,000
α	.72	.68	.64	.60	.56
β	.425	.400	.375	.350	.325
$\beta_1 = 2\beta$	.85	.80	.75	.70	.65
$\gamma = \alpha/\beta_1$	0.85	0.85	0.85	0.86	0.86

Table 2.3: Stress Block Coefficients

Thus, Equ. 2.7 (**ACI-318 10.2.7.3**) and the corresponding Fig. 2.5 are defined:

$$\begin{aligned} \beta_1 &= .85 && \text{if } f'_c \leq 4,000 \\ &= .85 - (.05)(f'_c - 4,000)\tfrac{1}{1,000} && \text{if } 4,000 < f'_c < 8,000 \end{aligned} \tag{2.7}$$

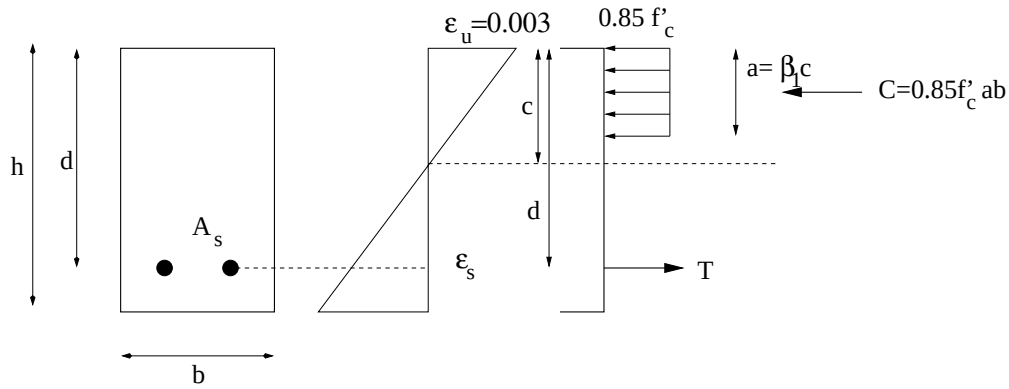

Figure 2.5: Whitney Stress Block

Failure can occur by either

yielding of steel: $\varepsilon_s = \varepsilon_y$; Progressive

crushing of concrete: $\varepsilon_c = .003$; Sudden; **(ACI 10.3.2)**.

For life-safety reasons it is preferred to have a failure through yielding in contrast to sudden crushing of the concrete, therefore, it is imperative that the stress-strain equilibrium is properly analyzed.

The most basic understanding about the differences between tension controlled sections and compression controlled sections are as follows:

Tension Failure:

$$\left.\begin{aligned} f_s &= f_y \\ A_s f_s &= .85 f'_c ab = .85 f'_c b \beta_1 c \\ \rho &= \tfrac{A_s}{bd} \end{aligned}\right\} c = \frac{\rho f_y}{.85 f'_c \beta_1} d \tag{2.8}$$

Compression Failure:

$$\varepsilon_c = .003 \tag{2.9}$$

$$\varepsilon_s = \frac{f_s}{E_s} \tag{2.10}$$

$$\frac{c}{d} = \frac{.003}{.003 + \varepsilon_s} \Rightarrow c = \frac{.003}{\frac{f_s}{E_s} + .003} d \tag{2.11}$$

Balanced Design:

Balanced design occurs if there is simultaneous yielding of the steel and crushing of the concrete. Hence, equating Equ. 2.11 and 2.8 results in the following:

$$\left.\begin{array}{rcl} \frac{\rho f_y}{.85 f'_c \beta_1} d & = & \frac{.003}{\frac{f_s}{E_s}+.003} d \\ \rho & = & \rho_b \end{array}\right\} \left.\begin{array}{rcl} \frac{\rho b f 2 d}{.85 f'_c \beta_1} & = & \frac{.003}{\frac{f_s}{E-s}+.003} d \\ E_s & = & 29,000\text{ksi} \end{array}\right\} \begin{array}{l} \rho_b = .85\beta_1 \frac{f'_c}{f_y} \frac{87{,}000}{87{,}000+f_y} \\ \textbf{(ACI 8.4.3)} \end{array} \tag{2.12}$$

To ensure failure by yielding,

$$\rho < .75\rho_b \tag{2.13}$$

ACI strength requirements

$$\begin{array}{rcll} U & = & 1.4D + 1.7L & \textbf{(ACI 9.2.1)} \\ U & = & 0.75(1.4D + 1.7L + 1.7W) & \textbf{(ACI 9.2.2)} \\ M_d = M_u & = & \phi M_n & \textbf{(ACI 9.1.1)} \\ \phi & = & .90 & \textbf{(ACI 9.3.2.2)} \end{array} \tag{2.14}$$

To account for temperature & shrinkage a minimum reinforcement ratio needs to be specified

$$\rho_{min} \geq \frac{200}{f_y} \qquad \textbf{(ACI 10.5.1)} \tag{2.15}$$

Note, that ρ need not be as high as $0.75\rho_b$. If steel is relatively expensive, or deflection is of concern, a lower ρ can be utilized. As a rule of thumb, if $\rho < 0.5\rho_b$, there is no need to check for deflection.

With the above terms defined, analysis of cross sections under both axial forces and moment can be computed.

2.4 Interaction Diagram

The interaction diagram of a beam-column's cross section defines the maximum combined axial load and applied moment that said beam-column section can undergo before the section begins to yield. Certain locations on the interaction diagram determine if the combined loading leads to a compression controlled failure, a tension controlled failure, or somewhere in-between the two. For

life safety, it is preferable to have such a section progressively fail in flexure rather than to have the section fail in a sudden crushing manner. For this reason the following load reductions ϕ are used **(ACI 9.3.2.1 & 9.3.2.2)**

Maximum Strain	Compression Controlled	Transition Region	Tension Controlled
Max Tensile Strain	$\varepsilon_s < .002$	$.002 \leq \varepsilon_s \leq .005$	$\varepsilon_s > .005$
Tied Columns	$\phi = .65$	$\phi = .65 + (\varepsilon_s - .002)\frac{250}{3}$	$\phi = .90$
Spiral Columns	$\phi = .75$	$\phi = .65 + (\varepsilon_s - .002)50$	$\phi = .90$

Table 2.4: Load Reduction Factors

The points in the interaction diagram are then computed using a series of strain distributions with the corresponding values of axial load and applied moment.

2.4.1 Interaction Diagram for Rectangular Cross Section

The analysis for a rectangular cross section uses the same principles and equations defined by the Whitney stress block method. Each point within the interaction diagram corresponds to a specific depth of the compression block within the cross section being analyzed. For rectangular uniaxial bending, the cross section dimensions remain constant as the neutral axis moves throughout the cross section, making it fairly simple in determining the resulting moments around the centroid. The tensile forces in the reinforcement can be computed by rearranging Equ. 2.11 into

$$\varepsilon_s = \frac{c-d}{c}\varepsilon_{cu} \tag{2.16}$$

With limiting values

$$-.002069 < \varepsilon_s < .002069 \tag{2.17}$$

The strain for each layer of steel is then compared to the yield strength of steel in compression and tension to account for the additional strength provided by both the compression and tensile steel. The summation of forces and corresponding the moments can subsequently be calculated by

multiplying the force of each component in the cross section by the distance around the centroid of the cross section Wight, J. K. and MacGregor, J. G. (2009).

$$P_{ns} = \sum_{i=1}^{n} f_s(i) A_s(i) \tag{2.18}$$

$$M_{ns} = \sum_{i=1}^{n} f_s(i) A_s(i)(Centroid - d(i)) \tag{2.19}$$

Where n is the number of layers of reinforcement in the section. f_s can be found as

$$f_s(n) = E\varepsilon_s(n) \tag{2.20}$$

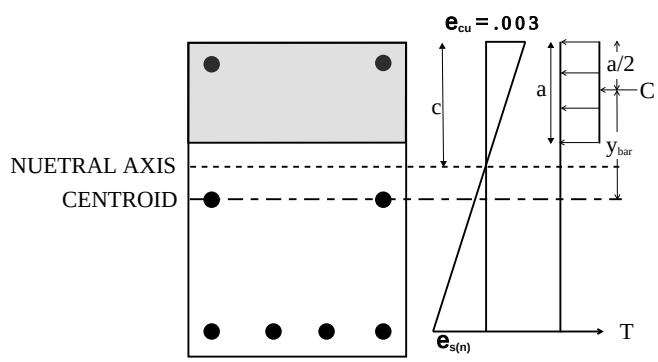

Figure 2.6: Forces in a Rectangular Cross Section

The term $\bar{y}$ is used to define the distance from the centroid of the compression block to the centroid of the cross section. Depending on the maximum tensile strain in the steel as defined in Table 2.4, the point corresponding to the appropriate depth of compression block can then be plotted. A detailed graphic of the stresses and strain in such a cross section is presented in Fig. 2.6

2.4.2 Interaction Diagram for Circular Cross Section

For circular cross sections, the determination of the area in compression and the moment arm of the compression block presents additional complexities involved with the irregular geometry. The area of the compression block is found by determining the angle theta from the point of the cross

section in ultimate compression to the point where the distance of the appropriate stress block coefficient multiplied by the neutral axis intersects the surface of the cross section, as depicted in Fig. 4.8

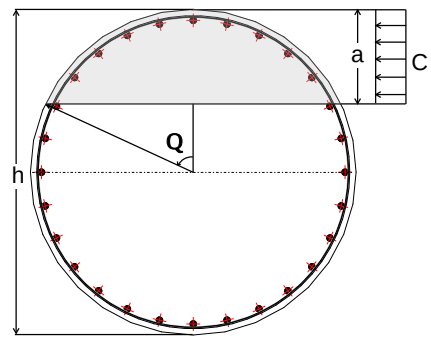

Figure 2.7: Determination of the Compression Block within a Circular Cross Section

The area is then found by:

$$A_{cn} = h^2 \left(\frac{\theta - sin\theta cos\theta}{4} \right) \tag{2.21}$$

The respective moment arm can be found as:

$$A\bar{y} = h^3 \left(\frac{sin^3\theta}{12} \right) \tag{2.22}$$

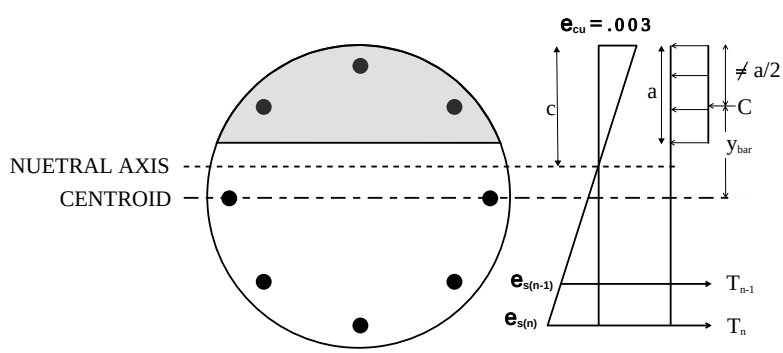

Figure 2.8: Forces in a Circular Cross Section

From here the axial forces and moments can the be found using the same procedure used for rectangular cross sections.

2.5 Mander's Stress-Strain Model

Typical design assumptions, including the Whitney Constant Stress Block, does not work as well when trying to obtain precise moment curvature relationships, as one of the main attractions to the Whitney model is that it slightly undervalues the cross-sectional strength of a column or beam. While a conservative design is preferable for the nominal strength of a beam-column, a more exact model is required in performing a pushover analysis. This is especially true for beam-columns, as the transverse reinforcement will provide additional compressive strength and ductility to the member that the traditional Whitney model will underestimate. The Mander stress-strain model is one of the first and most well known models currently used by AAS (2014). The Mander Model suggests that the moments and curvatures associated with the increase in flexural deformations of the member may be computed for various axial loads by increasing the curvature and satisfying the requirements of strain compatibility and equilibrium of forces. The method proposes that once the complete non-linear stress-strain curves are defined for both concrete and reinforcing steel, that a more accurate representation of the moment curvature relationship can be defined up until the ultimate strain of the member. What was at the time unique to Mander's model is the quantification of additional strength and ductility obtained by the confining effects of the transverse reinforcement. The ultimate strain is then defined as the point at which the transverse reinforcement yields, in turn eliminating the confinement effect on the core of the member, causing loss of all structural integrity. Mander's stress-strain equation for confined circular under monotonic loading is as follows:

$$f_c = \frac{f'_{cc} x r}{r - 1 + x^r} \tag{2.23}$$

Where f'_{cc} is the peak compressive strength of the confined concrete and ε_{cc} is the corresponding strain at said peak stress. The variables x and r can be defined as such:

$$x = \frac{\varepsilon_c}{\varepsilon_{cc}} \tag{2.24}$$

$$r = \frac{E_c}{E_c - E_{sec}} \tag{2.25}$$

$$\varepsilon_{cc} = \varepsilon_{co}\left[1 + 5\left(\frac{f'_{cc}}{f'_{co}} - 1\right)\right] \tag{2.26}$$

From here, f'_{co} and ε_{co} are defined as the unconfined concrete strength and corresponding strain, respectively. We also notice that Eq. 2.25 introduces the variable E_{sec}, or the secant modulus of confined concrete at peak stress, defined as Eq. 2.27. These variables are represented in Mander's stress-strain curve in Fig. 2.9

$$E_{sec} = \frac{f'_{cc}}{\varepsilon_{cc}} \tag{2.27}$$

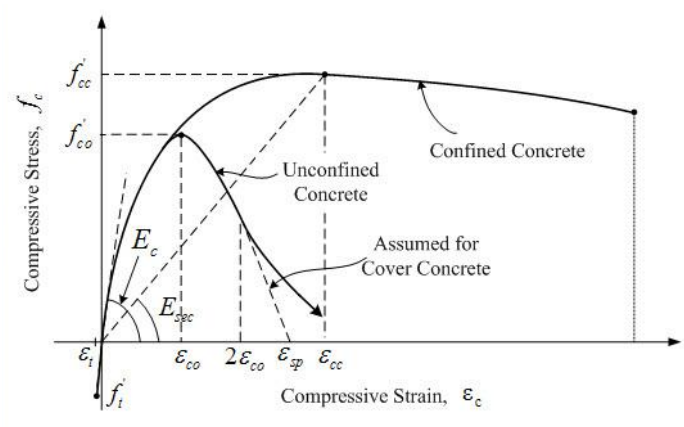

Figure 2.9: Manders Stress Strain Curve for Confined Concrete

2.5.1 Confined Circular Columns

The equations in Section 2.5 hold true for normal strength concrete, with the confinement strength dependent on the size and placement of the transverse reinforcement. For circular columns, either hooped ties or spiral cages can be implemented for transverse reinforcement. The max transverse pressure from the confining steel can only be applied efficiently to part of the concrete core where the confining stresses have fully developed due to arching between the levels of hoops/spirals. The area of ineffectively confined concrete will reach a maximum limit, and the area of effectively confined concrete will reach a minimum half way in-between these transverse layers. Fig. 2.10 gives a visual representation of the arching confinement Mander, J. B. and Priestley, M. J. N. and Park, R. (1988).

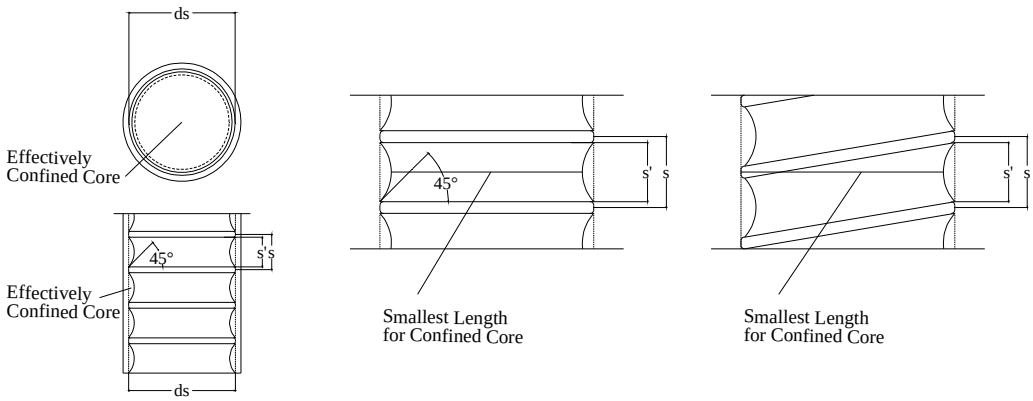

Figure 2.10: Effectively Confined Core for Circular Hoop Reinforcement

To properly address this arching action, the additional compression strength of the concrete provided by the transverse reinforcement takes into account the effective lateral confining stress f'_l as such:

$$f'_{cc} = f'_{co}\left(-1.254 + 2.254\sqrt{1 + \frac{7.94 f'_l}{f'_{co}}} - 2\frac{f'_l}{f'_{co}}\right) \tag{2.28}$$

Where f'_l can be defined as

$$f'_l = \frac{1}{2} k_e \rho_s f_{yh} \tag{2.29}$$

The variable k_e is the confinement effectiveness coefficient that can be defined as Eq. 2.30 for hooped reinforcement and Eq. 2.31 for spiral reinforcement, while ρ_s is defined as the ratio of the volume of transverse confining steel to the volume of confined concrete core for both hooped and spiral reinforcement given in Eq. 2.32:

$$k_e = \frac{\left(1 - \frac{s'}{2d_s}\right)^2}{1 - \rho_{cc}} \tag{2.30}$$

$$k_e = \frac{1 - \frac{s'}{2d_s}}{1 - \rho_{cc}} \tag{2.31}$$

$$\rho_s = \frac{A_{sp}\pi d_s}{\frac{\pi}{4}d_s^2 s} = \frac{4A_{sp}}{d_s s} \tag{2.32}$$

Where s is defined as the distance center to center between hoops or spirals, s' is defined as the clear distance between the radius of each set of hoops or pitch between the spirals, d_s is the diameter between bar centers, ρ_{cc} is the ratio of area of longitudinal reinforcement to the area of the core of the section enclosed by the radius to the center-line of the transverse reinforcement, and A_{sp} is the cross-sectional area of the transverse bar. With the ultimate confined compressive strength known, a stress-strain diagram can be developed up until the ultimate strain of the column. The ductility of the structure may be defined as the ability to undergo deformations without a substantial loss in flexural capacity of a member, Olivia, M. and Mandal, P. (2005). The available ductility of a structure is strongly influenced by the ultimate rotational capacity of the cross sections within a structure. The Mander Model defines this ultimate strain as the point where the longitudinal stresses causes the hooped/spiral reinforcement to fracture, rendering the compressive strength of the confined concrete ineffective Mander, J. B. and Priestley, M. J. N. and Park, R. (1988). Mander proposed an approach to find limiting strain utilizes an energy balance method where the increase in strain energy at column failure resulting from confinement can be provided by the strain energy capacity of the confining reinforcement as it yields in tension. By equating the ultimate strain energy capacity of the confining reinforcement per unit volume of the concrete core (U_{sh})

to the difference in area between the confined (U_{cc}) and unconfined (U_{co}) concrete strain curves, plus additional energy required to maintain yield in the longitudinal steel in compression (U_{sc}), the longitudinal concrete compressive strain corresponding to hoop fracture can be calculated by the following formulation.

$$U_{sh} = U_{cc} + U_{sc} - U_{co} \tag{2.33}$$

Which can be further defined as

$$\rho_s A_{cc} * \int_0^{\varepsilon_{sf}} f_s d\varepsilon_s = A_{cc} * \int_0^{\varepsilon_{cu}} f_c d\varepsilon_c + \rho_{cc} A_{cc} * \int_0^{\varepsilon_{cu}} f_{sl} d\varepsilon_c - A_{cc} * \int_0^{\varepsilon_{sp}} f_c d\varepsilon_c \tag{2.34}$$

Where A_{cc} is the area of confined core, ε_{sf} is the fracture strain of transverse steel, f_{sl} is the stress in longitudinal reinforcement, and ε_{sp} is the spalling strain of the unconfined concrete. To simplify Eq. 2.34 Mander's experimental data suggested that U_{sh} and U_{co} could be further simplified for a wide range of steel grades and diameters. The integral on the left-hand side of Eq. 2.34 designates the total area under the stress-strain curve for the transverse reinforcement up to the fracture strain. Experimental data suggests that this integration is effectively independent of bar size or yield strength and can be taken as:

$$\int_0^{\varepsilon_{sf}} f_s d\varepsilon_s = U_{sf} = 110Mpa = 15.954Ksi \tag{2.35}$$

The integral on the furthest right-hand side of Eq. 2.33 represents the area under the stress-strain curve for unconfined concrete. It was found through analysis of data collected prior to Mander's work that this integral can be approximated as:

$$\int_0^{\varepsilon_{sp}} f_c d\varepsilon_c = 0.017\sqrt{f'_{co}}Mpa = .006474\sqrt{f'_{co}}Ksi \tag{2.36}$$

These two simplifications bring us to the final form of our energy equation that can be used to solve for the ultimate strain of the confined concrete within the column.

$$\int_0^{\varepsilon_{cu}} f_c d\varepsilon_c + \int_0^{\varepsilon_{cu}} f_{sl} d\varepsilon_c = 15.954\rho_s + .006474\sqrt{f'_{co}} \tag{2.37}$$

To solve for ε_{cu}, the stress-strain relationship for the steel reinforcement must first be defined. From Chapter 8 of ASSHTO, the stress-strain relation and corresponding variables for ASTM A706 and A615 steel are found. Both types of steel follow the model in Fig. 2.11 AAS (2014).

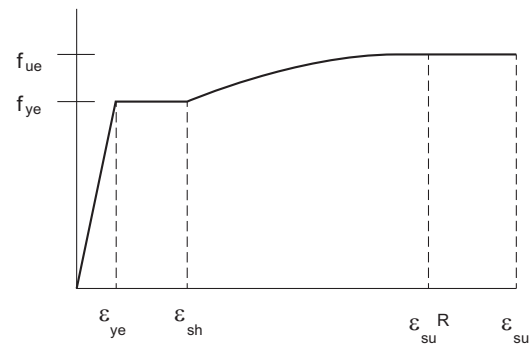

Figure 2.11: Reinforcing Steel Stress-Strain Model

Once the strain variables have been defined, we can partition the steel stress-strain curve into four distinct formulas. The first branch being the linear-elastic incline where

$$f_s = E_s \varepsilon_s \tag{2.38}$$

From here the steel goes through a yielding process where the stress is constant over a plastic deformation stretching between ε_{ye} and ε_{sh} as such

$$f_s = f_y \tag{2.39}$$

Once the strain hardening begins, Mander (1994) defines f_s as

$$f_s = f_{su} + (f_y - f_{su}) \left| \frac{\varepsilon_{su} - \varepsilon_s}{\varepsilon_{su} - \varepsilon_{sh}} \right|^p \tag{2.40}$$

Where the variable p is defined as

$$p = E_{sh} \frac{\varepsilon_{su} - \varepsilon_{sh}}{f_{su} - f_y} \tag{2.41}$$

And where E_{sh} is the tangent strain hardening modulus of elasticity taken as

$$E_{sh} = \frac{f_{ye}}{\varepsilon_{sh}} \tag{2.42}$$

The fourth section of the stress-strain curve is the final yielding of the steel where $f_s = f_{ue}$. In order to obtain ε_{cu}. The summation of integrals can then be utilized to find the ultimate compressive strain provided by the transverse reinforcement.

The strain energy theory presented above can be a little complex for the practicing engineer and as a result is not a required methodology in the accepted Pushover design methodology. About a decade after Mander's report on Theoretical Stress-Strain Model was published, a contributing author and colleague to Mander, M.J.N. Priestly, developed an equation that greatly simplified the process to define the ultimate compression strain, given as:

$$\varepsilon_{cu} = .004 + \frac{1.4\rho_s f_{yh}\varepsilon_{su}}{f'_{cc}} \tag{2.43}$$

This is a conservative estimate for the ultimate compressive strain and tends to underestimate by at least 50% Priestley, M.J.N. and Seible, F. and Calvi, G.M. (1996). Eq. 2.43 is the method that will be used in developing the pushover design tool presented later in this Report.

2.5.2 Confined Rectangular Columns

For rectangular columns, hooped ties are used for transverse reinforcement. As with circular reinforcement, the max transverse pressure from the confining steel can only be applied effectively to part of the concrete core where the confining stresses have fully developed. Arching now occurs between the levels of ties as well as between confined longitudinal reinforcement. Fig. 2.12 gives a visual representation of the arching action that takes place.

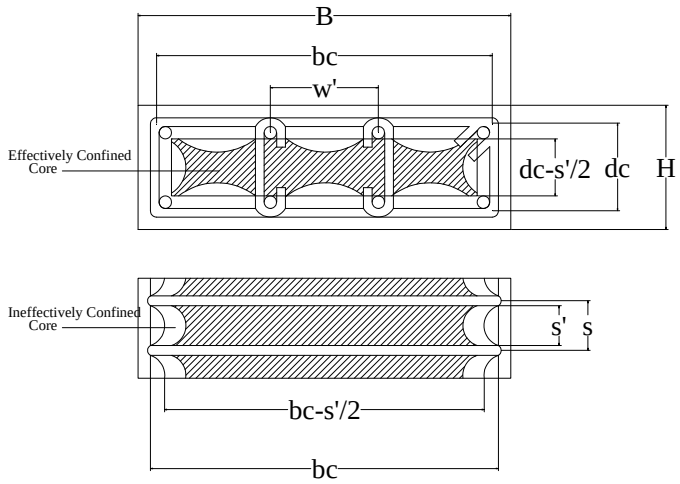

Figure 2.12: Effectively Confined Core for Rectangular Hoops

Notice in Fig. 2.12 that the width w' is defined as the width between longitudinal reinforcement confined in both the X and Y axis. The confinement effective coefficient for rectangular hoops can be defined as:

$$k_e = \frac{\left(1 - \sum_{i=1}^{n} \frac{\left(w_i'\right)^2}{6b_c d_c}\right)\left(1 - \frac{s'}{2b_c}\right)\left(1 - \frac{s'}{2d_c}\right)}{1 - \rho_{cc}} \tag{2.44}$$

Recall that with a circular cross section, the confining stress is consistent in both the X and Y axis as a result of geometry. To analyze a cross section with varying X and Y dimension, differing lateral confining stresses may be present between opposing axis will need to be taken into account. The differing values can be expressed as:

$$\rho_x = \frac{A_{sx}}{sd_c} \tag{2.45}$$

$$\rho_y = \frac{A_{sy}}{sb_c} \tag{2.46}$$

Where A_{sx} and A_{sy} are the total area of transverse reinforcement running in the X and Y direction respectively. The effective lateral confining stress can then be defined as:

$$f_{lx} = k_e \rho_x f_{yh} \tag{2.47}$$

$$f_{ly} = k_e \rho_y f_{yh} \tag{2.48}$$

The differing lateral confinement strengths lead to the use of a constitutive model involving these two lateral strengths in combination with the compressive in the Z axis. This method defined as the "five-parameter" multiaxial stress procedure is introduced as the theoretical method in determining the confined compressive of our confined core, resulting in a graphic-design tool presented in Fig. 2.13.

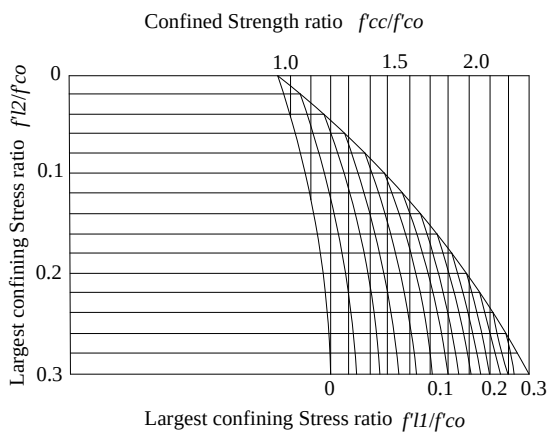

Figure 2.13: Effectively Confined Core for Rectangular Hoops

In the interest of procuring a design tool that will automatically determine the confined strength, the numerical procedure used to develop Fig. 2.13 is utilized. The 2 lateral confining stresses are converted from positive to negative values to represent the major and intermediate principle stresses such that:

$$\sigma_1 = -f_{l1} \tag{2.49}$$

$$\sigma_2 = -f_{l2} \tag{2.50}$$

Where f_{l1} is the larger of the two stresses, and f_{l2} is the lesser. The minor principal axis σ_3 can then be estimated as the unconfined strength of the concrete f'_c. It should be noted that this method is an iterative process where σ_3 converges to f'_{cc}. From here octahedral stresses can be found:

$$\sigma_{oct} = \frac{1}{3}\left(\sigma_1 + \sigma_2 + \sigma_3\right) \tag{2.51}$$

$$\tau_{oct} = \frac{1}{3}\left[\left(\sigma_1 - \sigma_2\right)^2 + \left(\sigma_2 - \sigma_3\right)^2 + \left(\sigma_3 - \sigma_1\right)^2\right]^{\frac{1}{2}} \tag{2.52}$$

$$cos\theta = \left(\frac{\sigma_1 - \sigma_{oct}}{\sqrt{2}\tau_{oct}}\right) \tag{2.53}$$

From here, the ultimate strength meridian surfaces, T and C, are found using the following equations derived by Elwi, A.A. and Murry, D.W. from data procured by Schickert and Winkler Mander, J. B. and Priestley, M. J. N. and Park, R. (1988).

$$T = 0.069232 - 0.661091\bar{\sigma}_{oct} - 0.04935\bar{\sigma}_{oct}^2 \tag{2.54}$$

$$C = 0.122965 - 1.150502\bar{\sigma}_{oct} - 0.315545\bar{\sigma}_{oct}^2 \tag{2.55}$$

Where:

$$\bar{\sigma}_{oct} = \frac{\sigma_{oct}}{f'_c} \tag{2.56}$$

The octohedral shear stress can then be found as defined by Willam, K. J. & Warnker (1975):

$$\bar{\tau}_{oct} = C\frac{\frac{.5D}{cos\theta} + \left(2T - C\right)\left(D + 5T^2 - 4TC\right)^{\frac{1}{2}}}{D + \left(2T - C\right)^2} \tag{2.57}$$

Where

$$D = 4\left(C^2 - T^2\right)cos^2\theta \tag{2.58}$$

$$\tau_{oct} = \bar{\tau}_{oct}f'_c \tag{2.59}$$

From here σ_3 can be recalculated as such:

$$\sigma_3 = \frac{\sigma_1 + \sigma_2}{2} - \sqrt{4.5\tau_{oct}^2 - 0.75\left(\sigma_1 - \sigma_2\right)^2} \tag{2.60}$$

Multiple iteration of this method will lead to σ_3 converging onto f'_{cc}.

2.6 Pushover Analysis

This section focuses on the derivations and methods used to develop the moment curvatures and subsequent plastic moments that are used to define under what conditions a plastic hinge will form. As previously mentioned, the interaction diagrams resulting from the Whitney stress block defines the maximum moment-axial combination in when $\varepsilon_{cu} = .003$ Conversely in the moment curvature analysis, the strain at the most extreme fiber of compression is increased from the initial strain, due to the constant axial load, to ε_{cu} defined by Eq. 2.43 for a particular axial load applied to the cross section. With the combination of the strain and axial load known, the neutral axis can be found, which subsequently yields the moment at each particular strain. The curvature can then be defined as the strain divided by the depth of the compression zone. Each strain will yield a specific curvature and corresponding moment which can be plotted to find the plastic moment of section, or the moment required to form a plastic hinge. AASHTO uses the following Fig. 2.14.

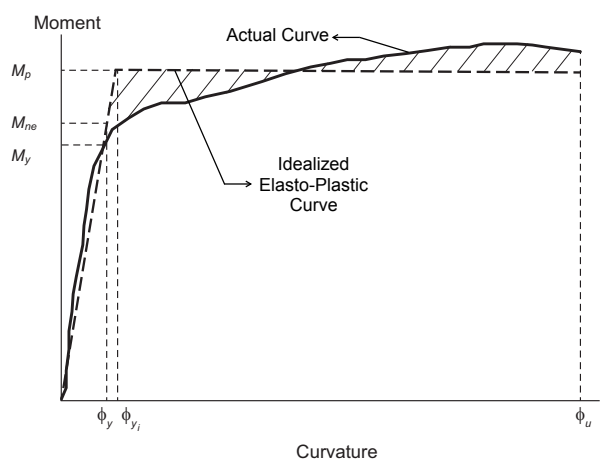

Figure 2.14: Moment Curvature Plot for a Particular Axial Load

The plastic moment is found after the yielding of the longitudinal reinforcement and is calculated as the moment at which the sum of the areas between the plastic moment and the moment curvature curve equal zero. The first step in developing the real curve in Fig.2.14, is to find the moment the corresponds to each incremental strain value.

2.6.1 Moment Curvature

The internal forces of the cross section resisting a selected axial load and strain at the most extreme fiber in compression will be composed from a combination of concrete compressive forces and tensile forces. To solve for the depth of the compression zone, and subsequently the moment capacity of the section, the depth of the compression zone will have to be found by iteration. The interaction between the compressive and tensile forces will change in a non-linear fashion as the depth of the compression zone is increased from 0 to the point at which the resulting combined forces in the concrete and steel reach that of the applied load. The moment can then be found as the resulting forces summed around the instant centroid of the section.

2.6.1.1 Instant Centroid

The first step in determining the moment curvature for a cross section with a constant axial load is to determine the neutral axis solely under compression forces. This point is known as the instant centroid of the cross section. For a symmetrical cross section with a symmetrical longitudinal reinforcement detailing, we can assume that the neutral axis under any axial load will be half of the distance from the most extreme fiber in compression to the end of the diameter or height of the cross section, for circular or rectangular cross sections respectively. For a beam-column with unsymmetrical reinforcement detailing, the neutral axis will increase or decrease with the change in axial compression. To determine the instant centroid, the following equations can be derived from equilibrium:

$$P = f_{ci}A_c + f_{si}A_s \tag{2.61}$$

Where f_{ci} and f_{si} can be solved for by

$$f_{ci} = \frac{f'_{cc}\left(\frac{\varepsilon_{ci}}{\varepsilon_{co}}\right)r}{r - 1 + \left(\frac{\varepsilon_{ci}}{\varepsilon_{co}}\right)^r} \tag{2.62}$$

$$f_{si} = E_s\varepsilon_{ci} \tag{2.63}$$

Where ε_{ci} can then be solved for as the one unknown variable in Eq. 2.61. The location of the neutral axis from the top of the most extreme fiber in compression can then be found as

$$IC = \frac{f_{ci}A_c\frac{h}{2} + \sum_{i=1}^{n} A_s\left(i\right) f_{si} d\left(i\right)}{f_{ci}A_c + \sum_{i=1}^{n} A_s\left(i\right) f_{si}} \tag{2.64}$$

Where n is the number of layers of reinforcement in the cross section.

2.6.1.2 Compression Zone

Given a certain depth of a compression zone and strain at the most extreme fiber in compression, the resulting compression forces can be found by numerically integrating under the concrete stress distribution curve. The compression zone for a rectangular section can be found as

$$C_c = \int_0^{\epsilon_{cm}} \left(\frac{f'_{cc}\left(\frac{\varepsilon_c}{\varepsilon_{co}}\right) r}{r - 1 + \left(\frac{\varepsilon_c}{\varepsilon_{co}}\right)^r} \right) \frac{A_{cn}}{\varepsilon_{cm}} d\varepsilon_c \tag{2.65}$$

Where A_{cn} is equal to $b * c$ for a rectangular section or 2.21 for a circular section. To analyze this solution numerically, the fifth order Gauss Quadrature rule can be implemented to obtain fairly accurate values for the resulting compression forces. Applying the Gaussian Quadrature rule then results in the following approximation

$$\int_0^{\varepsilon_{cm}} f\left(\varepsilon_c\right) \frac{A_{cn}}{\varepsilon_{cm}} d\varepsilon_c = \frac{\varepsilon_{cm} - 0}{2} \sum_{i=1}^{n} w_i f\left(\frac{\varepsilon_{cm} - 0}{2} x_i + \frac{\varepsilon_{cm} + 0}{2}\right) \frac{A_{cn}}{\varepsilon_{cm}} \tag{2.66}$$

Where f is the function from Eq. 2.65 with the points and weights defined as

Points x_i	Weights w_i
0	$\frac{128}{225}$
$\pm\frac{1}{3}\sqrt{5 - 2\sqrt{\frac{10}{7}}}$	$\frac{322+13\sqrt{70}}{900}$
$\pm\frac{1}{3}\sqrt{5 + 2\sqrt{\frac{10}{7}}}$	$\frac{322-13\sqrt{70}}{900}$

Table 2.5: Points and Weights for 5th Order Gauss Quadrature

2.6.1.3 Moment Arm

Once the resulting compressive force is determined, the distance to the centroid of the compressive force needs to be determined. Recall in Fig. 2.3, stress distribution profile changes as the maximum strain changes. Therefore, the distance to the centroid of the stress profile has be to be determined by iteration. This can be done given a fraction of ε_{cm} which can be labeled as ε_{bar}. The distance from the neutral axis to ε_{bar} can then be used to find the area in compression and the subsequent compressive forces that correspond to ε_{bar}. By assuming a relatively small value for ε_{bar} and iteratively increasing said value, the strain and distance c_{bar} that accounts for the depth of half the compressive force C can be found. The c_{bar} value at this point can then be defined as the distance to the centroid of the of the full compression zone, which can be used to find the moment arm y_{bar} of the full compression zone.

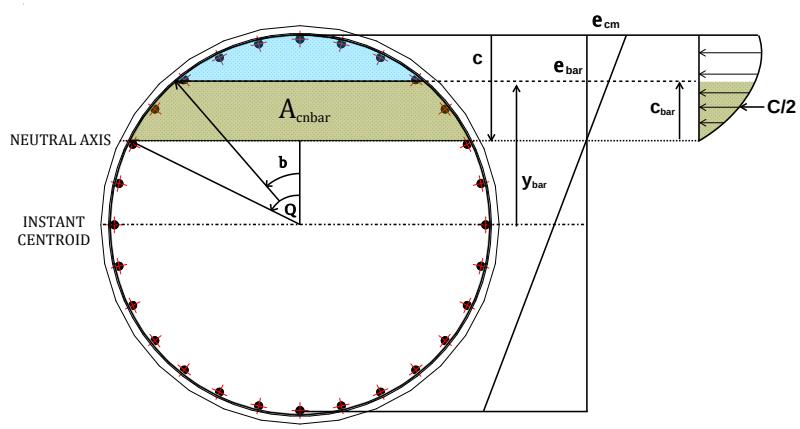

Figure 2.15: Moment Curvature Plot for a Particular Axial Load

The area in compression defined by c_{bar} can be defined as

$$A_{cnbar} = h^2\left(\frac{\theta - sin\theta cos\theta}{4}\right) - h^2\left(\frac{\beta - sin\beta cos\beta}{4}\right) \tag{2.67}$$

With the resulting compression force equal to the following using the Gaussian Quadrature rule.

$$C_{cbar} = \int_0^{\epsilon_{bar}} \left(\frac{f'_{cc}\left(\frac{\varepsilon_c}{\varepsilon_{co}}\right) r}{r - 1 + \left(\frac{\varepsilon_c}{\varepsilon_{co}}\right)^r}\right) \frac{A_{cnbar}}{\varepsilon_{bar}} d\varepsilon_c \tag{2.68}$$

From here we can define the axial loads and moments using the same methodology stated in Section 2.4. The same procedure is applicable to rectangular cross sections, with the only change being A_{cnbar} that becomes $c_{bar} * b$ This process is repeated using incremental values for ε_{cm} up until the ultimate strain of the cross section is reached, resulting in a plot similar to Fig. 2.14.

2.6.2 Plastic Moment

For the purpose of design, the moment curvature curve shall be idealized with an elastic perfectly plastic response to estimate the plastic moment capacity of a member's cross section. The elastic portion of the idealized curve shall pass through the point at which the first longitudinal reinforcing bar yields. The idealized plastic moment capacity can then be obtained for a particular axial load by equating the areas between the actual and idealized moment curvature curve, as previously shown in Fig. 2.14. The results from this analysis are used to establish the rotational capacity of plastic hinges as well as the associated plastic deformations. The process of using the moment curvature sectional analysis to determine the lateral load displacement relationship of a frame, column, or pier is defined as a pushover analysis.

2.6.3 Implementation of the Static Method

This section focuses on the formation of hinges within a structure and how the stiffness and geometric matrices are modified to account for the change in boundary conditions. There are two theorems in determining the point at which a plastic hinge may form, known as the Upper Bound and Lower Bound Theorems defined as such.

Upper Bound (Kinematic Analysis)

For an applied virtual displacement, the internal energy taken up by the structure on the assumption that the moment in every point where the curvature is changed equals the yielding moment and this energy is found to equal the work performed by the applied load for the same increment of deformation. This means that the resistance calculated for a kinematically admissible mechanism will be less than or at best equal to the required

resistance, resulting in collapse of the structure. This method does not produce the order in which hinges form, but rather assumes the simultaneous presence of all potential hinges required for collapse conditions.

Lower Bound (Static Analysis)

For an applied load, it is possible to find a moment field that fulfills all equilibrium conditions and the moment at no point is greater than, or at best equal to the yield moment, then the applied load is a lower bound value of the carrying capacity. This method produces the order in which hinges form and as such is appropriate for the design.

The Lower Bound Theorem is implemented in during the pushover analysis as it is important to define where and when plastic hinges form throughout the structure being analyzed. The Lower Bound Theorem can be carried out in one of two ways. For a linear elastic system, internal forces and moments within a structure increase linearly with a linear increase of load. Knowing this,

(1) An initial load can be applied to the structure, and corresponding moments can be calculated

(2) The largest moment is identified and set to equal the plastic moment by which the load required for the first hinge formation is found.

(3) The structure geometry is redrawn accounting for the formation of the new hinge. A new load is applied, and the resulting internal moments are found.

(4) The largest moment is identified and set equal to the plastic moment less the moment at said location from the previous analysis, by which the load required for the second hinge formation is found as the combine first and second load.

(5) The process is repeated until a mechanism is formed within the structure.

This method allows one iteration per hinge formation and is the most efficient way to define the formation of hinges when performing the analysis. The second method works in much the same

way, but is defined as a time history analysis, requiring multiple iterations between each hinge formation.

(1) An initial load can be applied to the structure, and corresponding moments can be calculated

(2) The load is incrementally increased by a predefined amount until the resulting moments match the value of a plastic hinge within the structure.

(3) The structure geometry is redrawn accounting for the formation of the new hinge. A new load is applied and incrementally increased until a second hinge forms as a result of the combined loading.

(4) The process is repeated until a mechanism is formed within the structure.

The advantage to the numerical time history analysis is that geometric non-linearity, or "P-Delta effects", can be accounted for during the analysis. Certain displacements under design loads will dictate whether or not P-Delta effects will significantly influence structural response, to be discussed in further detain in Section 2.8.1.

2.6.4 Hinge Formation & Analysis Using The Direct Stiffness Method

The forces, displacements, internal forces, reactions, and hinge formations are most efficiently determined through the use of the direct stiffness method in matrix structural analysis. Recall that for a beam element, the stiffness matrix can be defined as

$$[\mathbf{k}^{beam}] = \frac{EI}{L^3}\begin{bmatrix} 12 & 6L & -12 & 6L \\ 6L & 4L^2 & -6L & 2L^2 \\ -12 & -6L & 12 & -6L \\ 6L & 2L^2 & -6L & 4L^2 \end{bmatrix} \tag{2.69}$$

2.6.4.1 Semi-Rigid Connections

Where the force displacement relations are given by $\mathbf{p} + \mathbf{NEF} = \mathbf{ku}$. The analysis of a beam element with a hinge follows the same methods required to analyze a beam element with a semi-rigid connection as shown in Fig 2.6.4.1.

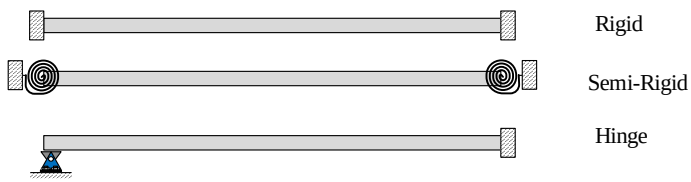

Figure 2.16: Members of Varying Rigidity

With semi-rigid connections, $\overline{\mathbf{p}} + \overline{\mathbf{NEF}} = \overline{\mathbf{k}}\overline{\mathbf{u}}$ is adopted to describe the force displacement relations.

To determine the stiffness for the beam element with semi-rigid connections in terms of $\mathbf{k}$, the following forces and displacements are defined in Eq. 2.70 and shown in Fig. 2.17

$$
\begin{aligned}
\lfloor p \rfloor &= \lfloor\ V_1 \quad M_2 \quad V_3 \quad M_4\ \rfloor \\
\lfloor \overline{p} \rfloor &= \lfloor\ \overline{V_1} \quad \overline{M_2} \quad \overline{V_3} \quad \overline{M_4}\ \rfloor \\
\lfloor u \rfloor &= \lfloor\ v_1 \quad \theta_2 \quad v_3 \quad \theta_4\ \rfloor \\
\lfloor \overline{u} \rfloor &= \lfloor\ \overline{v_1} \quad \overline{\theta_2} \quad \overline{v_3} \quad \overline{\theta_4}\ \rfloor
\end{aligned}
\tag{2.70}
$$

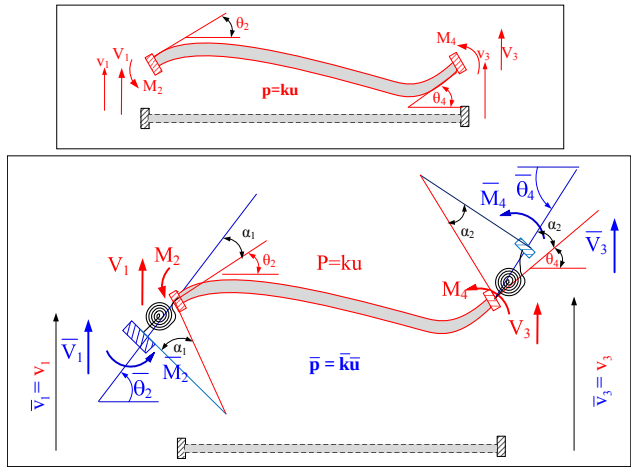

Figure 2.17: Semi Rigid Force Displacement Relations

Considering the free body diagram of the spring, and assuming that the springs are infinitesimally small, equilibrium requires that $\mathbf{p} = \overline{\mathbf{p}}$, resulting in

$$\left.\begin{aligned} v_1 &= \overline{v_1} \\ M_2 = k_1^s\left(\overline{\theta_2} - \theta_2\right); \theta_2 + \alpha_1 = \overline{\theta_2} \Rightarrow \theta_2 &= \overline{\theta_2} - \underbrace{\frac{M_2}{k_1^s}}_{\alpha_1} \\ v_3 &= \overline{v_3} \\ M_4 = k_2^s\left(\overline{\theta_4} - \theta_4\right); \theta_4 + \alpha_2 = \overline{\theta_4} \Rightarrow \theta_4 &= \overline{\theta_4} - \underbrace{\frac{M_4}{k_2^s}}_{\alpha_2} \end{aligned}\right\} \tag{2.71}$$

where k_1^s and k_2^s are the left and right spring rigidities respectively. By substituting v_1, v_2, θ_2 and θ_4 into $\mathbf{p} + \mathbf{NEF} = \mathbf{ku}$, the following set of coupled equations are developed.

$$\overline{V_1} + FV_1 = \frac{EI}{L^3}\left[12\overline{v_1} + 6L\left(\overline{\theta_2} - \frac{\overline{M_2}}{k_1^s}\right) - 12\overline{v_3} + 6L\left(\overline{\theta_4} - \frac{\overline{M_4}}{k_2^s}\right)\right] \tag{2.72}$$

$$\overline{M_2} + FM_2 = \frac{EI}{L^3}\left[6L\overline{v_1} + 4L^2\left(\overline{\theta_2} - \frac{\overline{M_2}}{k_1^s}\right) - 6L\overline{v_3} + 2L^2\left(\overline{\theta_4} - \frac{\overline{M_4}}{k_2^s}\right)\right] \tag{2.73}$$

$$\overline{V_3} + FV_3 = \frac{EI}{L^3}\left[-12\overline{v_1} - 6L\left(\overline{\theta_2} - \frac{\overline{M_2}}{k_1^s}\right) + 12\overline{v_3} - 6L\left(\overline{\theta_4} - \frac{\overline{M_4}}{k_2^s}\right)\right] \tag{2.74}$$

$$\overline{M_4} + FM_4 = \frac{EI}{L^3}\left[6L\overline{v_1} + 2L^2\left(\overline{\theta_2} - \frac{\overline{M_2}}{k_1^s}\right) - 6L\overline{v_3} + 4L^2\left(\overline{\theta_4} - \frac{\overline{M_4}}{k_2^s}\right)\right] \tag{2.75}$$

Equations can be uncoupled to express the forces exclusively in terms of the displacement.

To do this, Eq. 2.73 and 2.75 need to be solved simultaneously in terms of $\overline{u}$ resulting in

$$\begin{aligned}
\overline{M_2} &= \frac{EI}{L^3}\frac{\phi_b}{\Phi}\left[6L(2-\phi_2)\overline{v_1}+4L^2(3-2\phi_2)\overline{\theta_2}-6L(2-\phi_2)\overline{v_3}+2L^2\phi_2\overline{\theta_4}\right] \\
&\quad +\frac{\phi_1}{\Phi}\left[(4-3\phi_2)FM_2-2(1-\phi_2)FM_4\right] \qquad (2.76) \\
\overline{M_4} &= \frac{EI}{L^3}\frac{\phi_2}{\Phi}\left[6L(2-\phi_1)\overline{v_1}+2L^2\phi_1\overline{\theta_2}-6L(2-\phi_1)\overline{v_3}+4L^2(3-2\phi_1)\overline{\theta_4}\right] \\
&\quad +\frac{\phi_2}{\Phi}\left[-2(1-\phi_1)FM_2+(4-3\phi_1)FM_4-2(1-\phi_1)FM_2\right] \qquad (2.77)
\end{aligned}$$

where

$$\begin{aligned}
\phi_1 &= \frac{k_1^s L}{EI+k_1^s L} \\
\phi_2 &= \frac{k_2^s L}{EI+k_2^s L} \\
\Phi &= 12-8\phi_1-8\phi_2+5\phi_1\phi_2
\end{aligned}$$

ϕ can be defined as a "rigidity factor". For rigid connection $\phi = 1$, whereas for hinged ones $\phi = 0$.

Next Eq.2.76 and 2.77 can be substituted into Eq. 2.72 and 2.74 to obtain the final pieces of the stiffness matrix.

$$\begin{aligned}
\overline{V_1} &= \frac{EI}{\Phi L^3}\left[12(\phi_1+\phi_2-\phi_b\phi_2)\overline{v_1}+6L\phi_1(2-\phi_2)\overline{\theta_2}-12(\phi_1+\phi_2-\phi_1\phi_2)\overline{v_3}+6L\phi_2(2-\phi_1)\overline{\theta_4}\right] \\
&\quad +FV_1-\frac{6}{\Phi L}\left[(1-\phi_1)(2-\phi_2)FM_2+(1-\phi_2)(2-\phi_1)FM_4\right] \qquad (2.78) \\
\overline{V_3} &= \frac{EI}{\Phi L^3}\left[-12(\phi_1+\phi_2-\phi_b\phi_2)\overline{v_1}-6L\phi_1(2-\phi_2)\overline{\theta_2}+12(\phi_1+\phi_2-\phi_1\phi_2)\overline{v_3}-6L\phi_2(2-\phi_1)\overline{\theta_4}\right] \\
&\quad +FV_3+\frac{6}{\Phi L}\left[(1-\phi_1)(2-\phi_2)FM_2+(1-\phi_2)(2-\phi_1)FM_4\right] \qquad (2.79)
\end{aligned}$$

Combing the decoupled equations as $\left\{\overline{P}\right\}+\left\{\overline{NEF}\right\}=\left[\overline{k}\right]\left\{\overline{u}\right\}$, the following stiffness matrix can be found.

$$[\bar{\mathbf{k}}] = \frac{\mathbf{EI}}{\mathbf{\Phi L^3}} \begin{bmatrix} 12(\phi_1+\phi_2-\phi_1\phi_2) & 6L\phi_1(2-\phi_2) & -12(\phi_1+\phi_2-\phi_1\phi_2) & 6L\phi_2(2-\phi_1) \\ 6L\phi_1(2-\phi_2) & 4L^2\phi_1(3-2\phi_2) & -6L\phi_1(2-\phi_2) & 2L^2\phi_1\phi_2 \\ -12(\phi_1+\phi_2-\phi_1\phi_2) & -6L\phi_1(2-\phi_2) & 12(\phi_1+\phi_2-\phi_1\phi_2) & -6L\phi_2(2-\phi_b) \\ 6L\phi_2(2-\phi_1) & 2L^2\phi_1\phi_2 & -6L\phi_2(2-\phi_1) & 4L^2\phi_2(3-2\phi_1) \end{bmatrix} \tag{2.80}$$

For fully rigid connections, $\phi = 1$, the original stiffness matrix of the beam, Eq. 2.69, can be recovered,

By setting $\phi_1 = 0$ and $\phi_2 = 1$ a hinge is defined on the left end of the beam, and a rigid connection is defined on the right. By plugging into Eq. 2.80, the corresponding stiffness matrix becomes

$$[\bar{\mathbf{k}}] = \frac{\mathbf{EI}}{\mathbf{L^3}} \begin{bmatrix} 3 & 0 & -3 & 3L \\ 0 & 0 & 0 & 0 \\ -3 & 0 & 3 & -3L \\ 3L & 0 & -3L & 3L^2 \end{bmatrix} \tag{2.81}$$

By adding axial forces to the equation, it can be shown that the stiffness matrix of an individual beam column with similar boundary conditions is given by

$$[\bar{\mathbf{k}}] = \begin{bmatrix} AE/L & 0 & 0 & -AE/L & 0 & 0 \\ 0 & 3EI/L^3 & 0 & 0 & -3EI/L^2 & 3EI/L^2 \\ 0 & 0 & 0 & 0 & 0 & 0 \\ -AE/L & 0 & 0 & AE/L & 0 & 0 \\ 0 & -3EI/L^3 & 0 & 0 & 3EI/L^3 & -3EI/L^2 \\ 0 & 3EI/L^2 & 0 & 0 & -3EI/L^2 & 3EI/L \end{bmatrix} \tag{2.82}$$

From here, global structural equilibrium can be found through Eq. 2.83

$$\{\mathbf{P}\} = \{\mathbf{FEA}\} + [\mathbf{K}]\{\mathbf{\Delta}\} \tag{2.83}$$

Where [**k**]] is the global stiffness matrix, [**FEA**] is the equivalent nodal loads, and [**Delta**] is the vector of generalized nodal displacements. The equation can be broken down further into a system

that will allow for computation of unknown displacements, reactions, and internal forces within a structure given known loading and boundary conditions.

2.6.4.2 Direct Stiffness Method

The Direct Stiffness Method is implemented within ANPA. Through the use of the direct stiffness method, one can obtain the global stiffness matrix of continuous beam-column elements from assembling member stiffness matrices of individual beam elements. Beam elements are consistent between areas of similar cross sections, thus treating each span as an individual beam. The combined stiffness matrix for a structure, or the "augmented stiffness matrix" is found by organizing the combined matrix in such a way that the free degrees of freedom within the structure, $\mathbf{K_{tt}}$, are grouped separate from the restrained degrees of freedom, $\mathbf{K_{uu}}$, as shown in Eq. 2.89.

$$\left\{\frac{\mathbf{P_t}}{\mathbf{R_u}}\right\} = \begin{bmatrix} \mathbf{K_{tt}} & \mathbf{K_{tu}} \\ \mathbf{K_{ut}} & \mathbf{K_{uu}} \end{bmatrix} \left\{\frac{\mathbf{\Delta_t}}{\mathbf{\Delta_u}}\right\} \tag{2.84}$$

Displacements at the unrestrained degrees of freedom can then be found as Eq. 2.85

$$\mathbf{\Delta_t} = \mathbf{K_{tt}^{-1}}(\mathbf{P_t} - \mathbf{K_{tu}}\mathbf{\Delta_u}) \tag{2.85}$$

And the Reactions can be found as Eq. 2.86

$$\mathbf{R_u} = \mathbf{K_{ut}}\mathbf{\Delta_t} + \mathbf{K_{uu}}\mathbf{\Delta_u} \tag{2.86}$$

Special attention has to be taken when developing the augmented stiffness matrix as the formation of a hinge at a unrestrained degree of freedom will leave a zero along the diagonal of the $\mathbf{K_{tt}}$, resulting in an unsolvable Eq. 2.85. As such, both the load vector $\mathbf{P_t}$ and $\mathbf{K_{tt}}$ need to be condensed so that the rotational degree of freedom is excluded from the analysis.

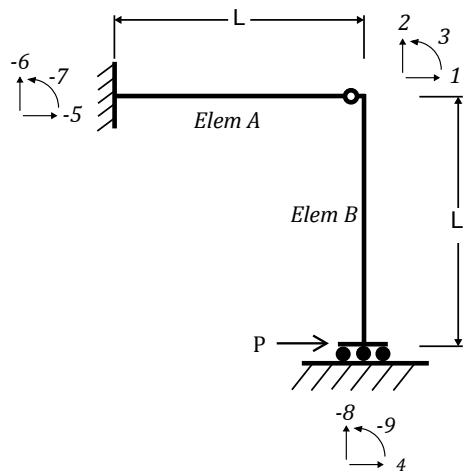

Figure 2.18: Two Identical Structures With and Without Hinge

A simplified way to analyze the hinge development is to assume that the hinge is located at the nodal location conjoining the two elements. Since it is probable that the two elements have differing moment capacities, the formation of a hinge in one element will have to be modeled to show the formation of a hinge at the conjoining node in the second element, essentially eliminating the stiffnesses contained in the third row/ third column of Eq. 2.88.

$$[\mathbf{k}^{(\mathbf{A})}] = \begin{array}{c} \\ -5 \\ -6 \\ -7 \\ 1 \\ 2 \\ 3 \end{array} \begin{array}{c} \begin{array}{cccccc} -5 & -6 & -7 & 1 & 2 & 3 \end{array} \\ \begin{pmatrix} A_{11} & A_{12} & A_{13} & A_{14} & A_{15} & 0 \\ A_{21} & A_{22} & A_{23} & A_{24} & A_{25} & 0 \\ A_{31} & A_{32} & A_{33} & A_{34} & A_{35} & 0 \\ A_{41} & A_{42} & A_{43} & A_{44} & A_{45} & 0 \\ A_{51} & A_{52} & A_{53} & A_{54} & A_{55} & 0 \\ 0 & 0 & 0 & 0 & 0 & 0 \end{pmatrix} \end{array} \tag{2.87}$$

$$[\mathbf{k}^{(\mathbf{B})}] = \begin{array}{c} \\ 1 \\ 2 \\ 3 \\ 4 \\ -8 \\ -9 \end{array} \begin{array}{c} \begin{array}{cccccc} 1 & 2 & 3 & 4 & -8 & -9 \end{array} \\ \begin{pmatrix} B_{11} & B_{12} & B_{13} & B_{14} & B_{15} & B_{16} \\ B_{21} & B_{22} & B_{23} & B_{24} & B_{25} & B_{26} \\ B_{31} & B_{32} & B_{33} & B_{34} & B_{35} & B_{36} \\ B_{41} & B_{42} & B_{43} & B_{44} & B_{45} & B_{46} \\ B_{51} & B_{52} & B_{53} & B_{54} & B_{55} & B_{56} \\ B_{61} & B_{62} & B_{63} & B_{64} & B_{65} & B_{66} \end{pmatrix} \end{array} \tag{2.88}$$

The Global Stiffness Matrix then contain eight total degrees of freedom, absent of any zeroes along the matrix axis as shown in Eq. 2.89.

$$[\overline{\mathbf{K}}] = \left[\begin{array}{ccc|cccccc} A_{44}+B_{11} & A_{45}+B_{12} & B_{14} & A_{41} & A_{42} & A_{43} & B_{15} & B_{16} \\ A_{54}+B_{21} & A_{55}+B_{22} & B_{24} & A_{51} & A_{52} & A_{53} & B_{25} & B_{26} \\ B_{41} & B_{42} & B_{44} & 0 & 0 & 0 & B_{45} & B_{46} \\ \hline A_{14} & A_{15} & 0 & A_{11} & A_{12} & A_{13} & 0 & 0 \\ A_{24} & A_{25} & 0 & A_{21} & A_{22} & A_{23} & 0 & 0 \\ A_{34} & A_{35} & 0 & A_{31} & A_{32} & A_{33} & 0 & 0 \\ B_{51} & B_{52} & B_{54} & 0 & 0 & 0 & B_{55} & B_{56} \\ B_{61} & B_{62} & B_{64} & 0 & 0 & 0 & B_{65} & B_{66} \end{array}\right] \tag{2.89}$$

For a more advanced analysis, it is recommended that the formation of a hinge be placed to one side or the other of the conjoining node. For the frame structure pictured in Fig. 2.18, the hinge within the structure is pictured on the right side of "Element A" a relatively small distance off from the location of the node that joins elements A and B. Since it is probable that the two elements have different plastic moment capacities, the model can be set up to analyze a plastic hinge in "Element A" a relatively small distance away from the conjoining node rather than assuming a perfectly plastic hinge at the nodal location that conjoins the two elements. This length away from the conjoining node is known as the plastic length of the element. Likewise, a separate hinge

in "Element B" can be analyzed in the same manner. The complexity of such an analysis calls for the development of a new element at the creation of each hinge. The proper way to model such a development would be to assign additional nodes, elements, and subsequent stiffness matrices during the iterative matrix structural analysis as incremental loads are applied.

2.7 Simplified Pushover Analysis Using AASHTO Hand Calculations

An alternative method for determining the displacement capacity of a structural system can be implemented for seismic design category D given the expected plastic moment and plastic curvature that a column will yield under. By following a few simple hand calculations, we can obtain the shear force required for the first hinge to form as well as the total displacement demand. This analysis is less conservative than the overly conservative pushover analysis described in Section 2.6. The real displacement capacity of the structure is said to lie in-between these two methods of analyses.

2.7.1 Shear Required For Hinge Formation

For a single beam-column element, the shear required for the first hinge can be calculated given the plastic moment values of the specified cross section. Assuming fix-fix boundary conditions, the moment diagram can be defined as shown in Fig. 2.19

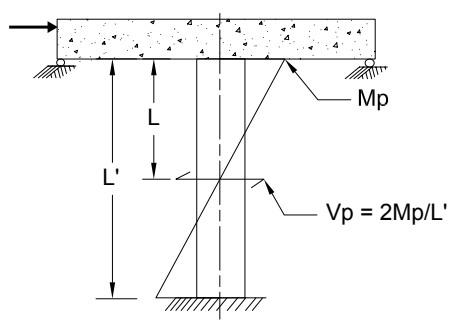

Figure 2.19: Moment Distribution over Height of Pier

Where

$$V_p = \frac{2M_p}{L'} \tag{2.90}$$

This calculation can also serve as a simple check to make sure that the results obtained from Section 2.6 are as expected.

2.7.2 Displacement Capacity

Individual member displacements are defined as the portion of global displacement attributed to the elastic column idealized displacement Δ_{yi} and plastic displacement demand Δ_{pd} of an equivalent member from the point of maximum moment to the point of contraflexure. AASHTO uses the following figure in determining these values.

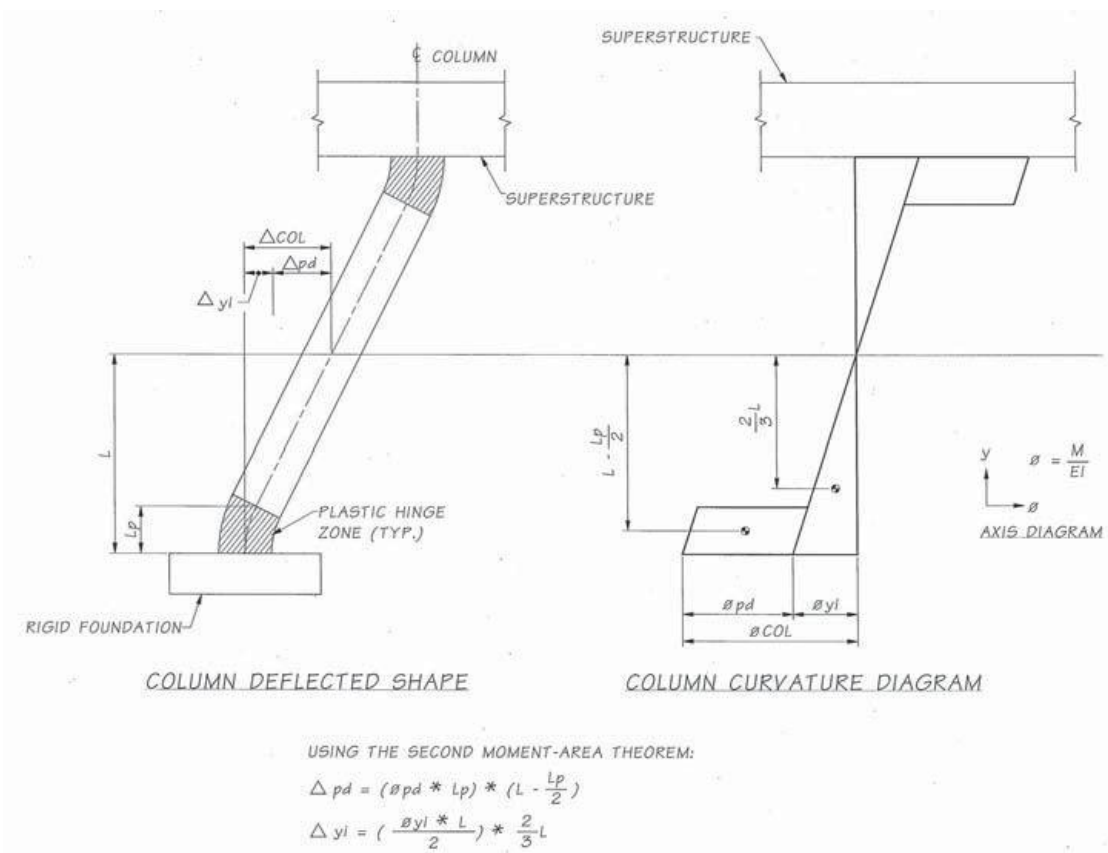

Figure 2.20: **(AASHTO Fig. C4.9-2)** Pier-Deflected Shape and Curvature Diagram

L_p is defined as the length of the plastic hinge. For a reinforced concrete column framing into a footing, an integral bent cap, an oversized shaft, or a cased shaft, the plastic hinge length, L_p in inches, can be calculated as

$$L_p = .08L + .15f_{ye}d_{bl} \geq .3f_{ye}d_{bl} \qquad \textbf{(AASHTO 4.11.6-1)} \tag{2.91}$$

Where L is defined as the length of the column from the point of maximum moment to the point of contraflexure in inches, d_{bl} is the diameter of longitudinal reinforcing steel. From here the elastic displacement can be found as

$$\Delta_e = \frac{\phi_{yi}L^2}{3} \qquad \textbf{(AASHTO C4.9-3)} \tag{2.92}$$

Where ϕ_{yi} is the idealized yield curve as shown in Fig. 2.21 and can be solved for as

$$\phi_{yi} = \frac{M_y}{EI} \tag{2.93}$$

$$M_y = \frac{V_pL}{2} \tag{2.94}$$

The plastic displacement capacity can then be found given the plastic curvature imposed by the design. Plastic curvature is defined as the delta between the elastic curvature and the rotational demand on the cross section, shown in Fig. 2.21

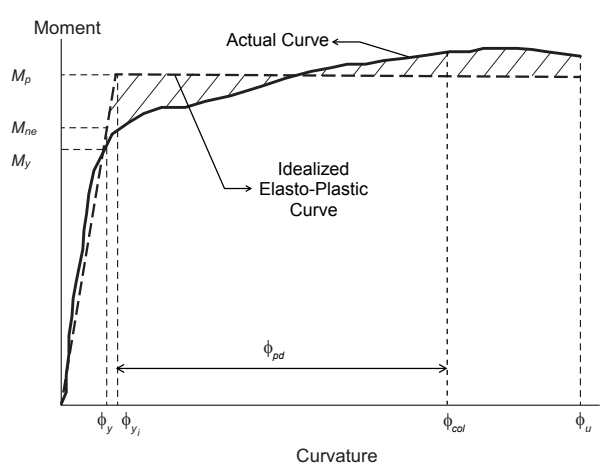

Figure 2.21: Moment Curvature Diagram with Plastic Curvature Demand

$$\Delta_{pd} = \phi_{pd} L_p \left(L - \frac{L_p}{2} \right) \qquad \textbf{(AASHTO C4.9-4)} \tag{2.95}$$

With the total displacement demand equating to:

$$\Delta_{Tot} = \Delta_{pd} + \Delta_e \tag{2.96}$$

2.8 Capacity Requirements

Checks are to be performed throughout both Pushover analyses presented above which will control the sizing of beam-columns and reinforcement detailing. Additional analyses outside the scope of the pushover analyses may need to be performed in the event that certain parameters are not met, specifically P-delta requirements.

2.8.1 P-Delta Check

Geometric non-linearity, or P-Delta Effects, may be ignored during the design process as long as the resulting moment due to the dead load and displacement is less than 25% of the plastic moment of the cross section, as shown in Eq. 2.97.

$$P_{DL} \Delta_r \leq .25 M_p \tag{2.97}$$

Where Δ_r is the relative lateral offset between the point of contraflexure and the furthest end of the plastic hinge in inches. The point of contraflexure in a cantilever column, assuming a fixed base, is equal to the total height of the column. If the design does not comply with Eq. 2.97, a few design actions can be taken including:

(1) increase the column moment capacity by adding additional longitudinal reinforcement,

(2) reconfigure the bridge to reduce the deal load demand acting on the column, or

(3) implement a non-linear time history analysis to explicitly consider P-Delta effects.

If the engineering chooses to perform a non-linear time history analysis, post-yield stiffness, stiffness degradation, and unloading stiffness models that are capable of capturing the expected structure response due to seismic-induced cyclic loading are required.

2.8.2 Moment Check

Since the pushover analysis is a static method used to describe the performance of a structure under dynamic loading, it is necessary to check that the moment capacity at the base of the structure can withstand the moments induced by the expected accelerations during a 1,033 year event. To perform this analysis, the induced shear, combined with the length between the point of contraflexure and the furthest end of the plastic hinge as described in Fig. 2.19, with the notation that V_{1033} is now

$$V_{1033} = C_s DL \tag{2.98}$$

Where DL is defined as the un-factored dead load of the structure. The moment can then be taken as

$$M_{1033} = V_{1033} \frac{L'}{2} \tag{2.99}$$

As long as the moment induced by a 1033 year event is less than the plastic moment of the column at the section of interest, the column will have adequate moment capacity.

2.9 Conclusion

It is evident that a pushover analysis requires a multitude of factors that need to be taken into consideration throughout the design process. The sections above shows how the displacement demands are determined through spectral analyses, how the displacement capacity is found through an analysis of the sections and elements within a structure, and how the formation of plastic hinges are modeled through the use of the direct stiffness method. While a pushover analysis can be

preformed through the use of hand calculations, it is advised that the more intricate method using a static analysis be performed, as this will yield more conservative displacement capacity results.

Chapter 3

Matlab Implementation

3.1 Introduction

The implementation of the Matlab program ANPA is discussed in what design steps are taken in order to assist the practicing engineer through the design of a pushover analysis. The analysis is broken down into three sections consisting of the Spectral Analysis, the Moment Curvature/Plastic Moment Analysis, and the Structural Analysis. Fig. 3.1 depicts the loops that ANPA performs in determining the cross sections, elements, and subsequent hinge formations throughout the analysis. Circular cells mark the beginning and end of an analysis, while the rectangular cells mark an internal process within the program. The lozenge cells, or diamond-shaped cells, mark a decision within the analysis that will result in either a "yes" or "no" answer. The rectangular cells highlighted in yellow are shown with more detail in the following subsections. The notation for variables found throughout this chapter correlate with the equations defined in Chapter 2. Development of flowcharts specifically covering the elementary Beam-Column Interaction Analysis and Direct Stiffness Analysis were not pursued.

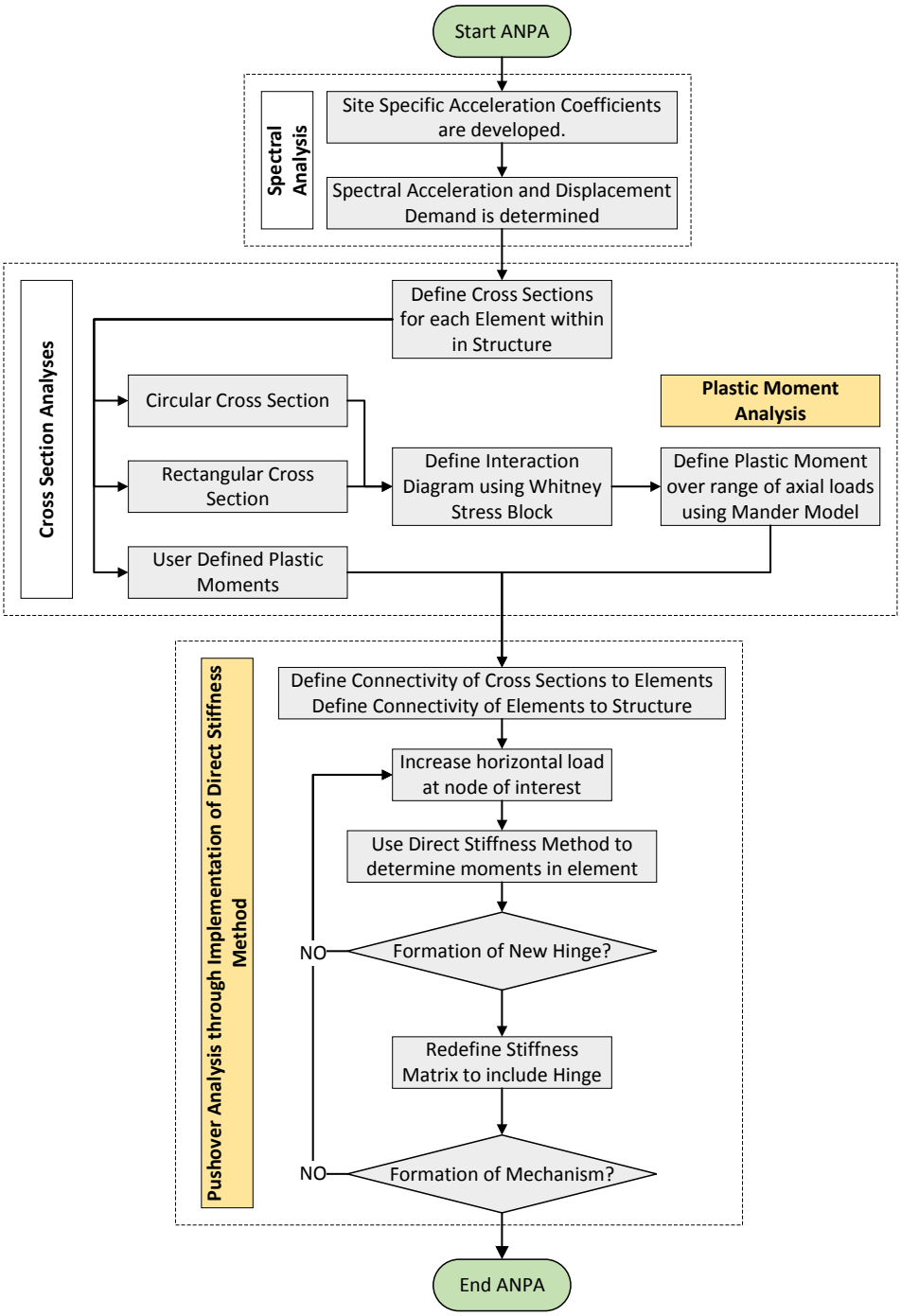

Figure 3.1: Main Program Flowchart

3.2 Plastic Moment

The steps required to determine the plastic moment for each subsequent axial load require multiple iterations that vary with the precision of the prescribed strain increments. As discussed in Chapter 2, a range of strains located at the face of the cross section maximum compression will determine the plastic moment. A parametric study discussing the advantages and disadvantages of variable strain increments can be found in Appendix A. There are two main loops within the analysis shown in Fig. 3.2 that account for most of the computational time. One of the main loops is the calculation of the moment arm. Since the stress-strain curve of the concrete will vary with the axial load applied to the cross section, the moment arm of the concrete in compression will vary between each loop. The second main loop contained in this analysis defines the compression or tension in the longitudinal steel reinforcement. It is important to note that while the calculation of the confined compressed concrete takes into account the non-linearity of the steel, the strain compatibility loop does not. The strength of the steel is capped at the corresponding yield strain of the steel in both compression and tension. While this conceptual assumption is admissible for this analysis, the non-linearity of the steel would have to be taken into account if P-Delta effects are to be considered. Once the maximum prescribed axial load has been reached, the analysis for the cross-section of interest ends. If there is more than one cross section to be analyzed, this process is repeated for the parameters defined by the input file.

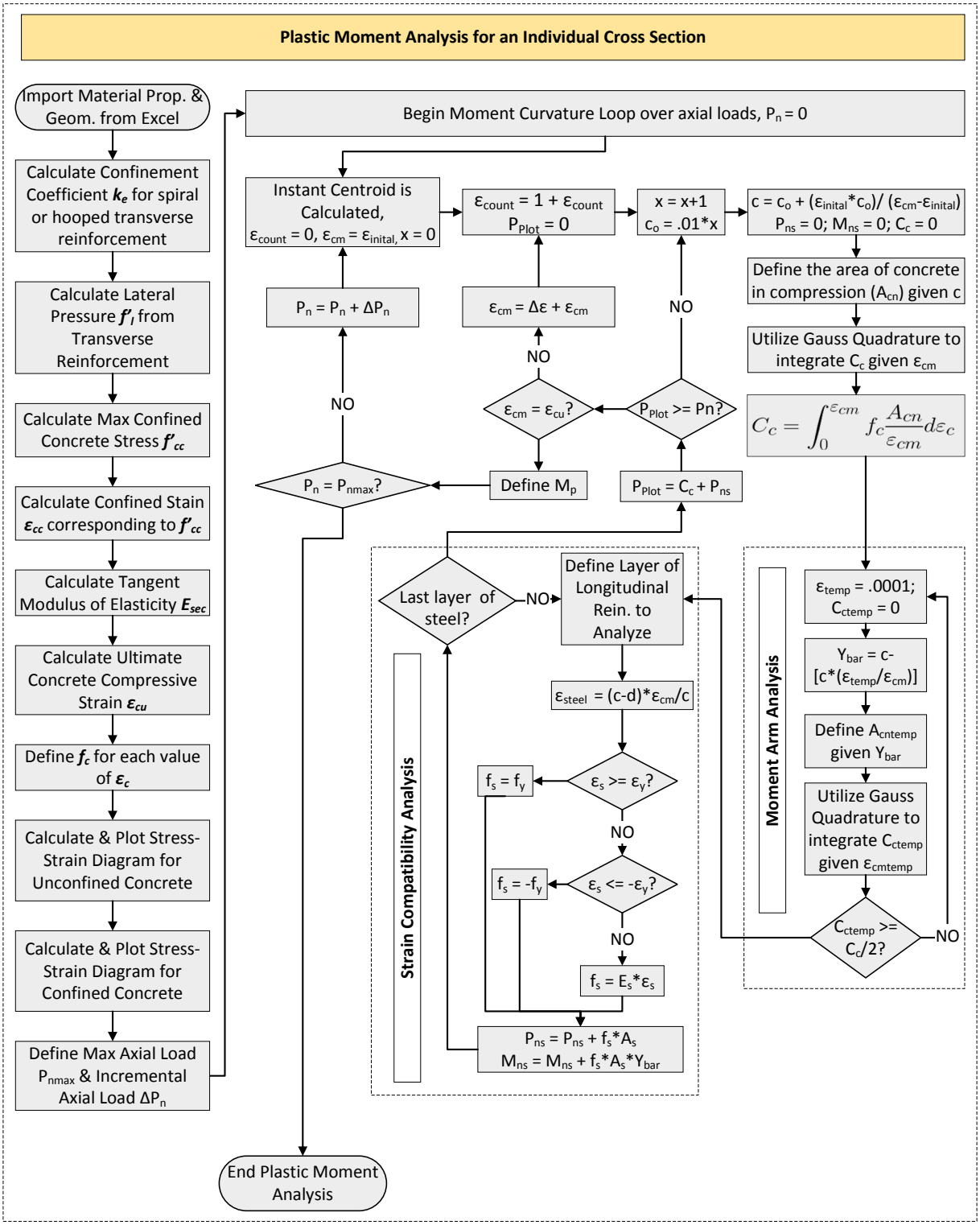

Figure 3.2: Moment Curvature/ Plastic Moment Analysis Flowchart

3.3 Pushover

The steps required to determine the order in which plastic hinges form within the structure is a bit more succinct than the process to define the plastic moments. Plastic Moments and corresponding axial loads are assigned to each end of a single element within the structure and internal moments within the structure are checked to determine at what point the internal moment surpasses the plastic moment. Data Structures are created and overwritten during each loop that contain the displacements, reactions, and internal forces corresponding to each applied incremental load. A target hinge count "q" is set so that the data structure is saved when the number of hinges within the structure reach the target count, ie: when H = q. This process denotes a prior data structure as that of the previous hinge formation. The program ends once a mechanism is formed within the structure, or more simply put, when any part of the structure is free to rotate. This is checked by calculating the condition number of K_{tt}. The condition number can be defined as the ratio of the largest singular value to the smallest within a matrix. Since there is no stiffness to a hinge, this number will extrapolate to values well above 10^{15} when a mechanism is present. Once this value is reached, the loop is exited and the pushover analysis is complete.

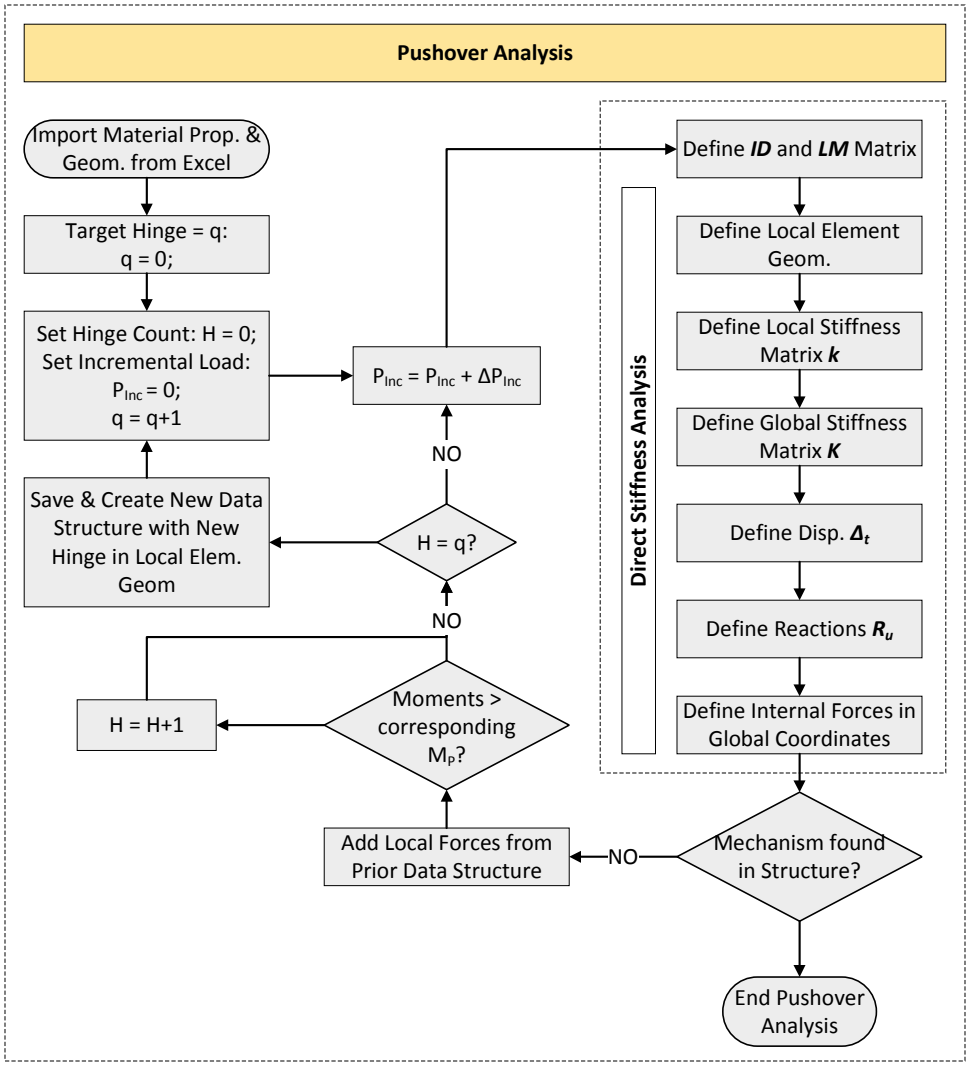

Figure 3.3: Pushover Matrix Structural Analysis Flowchart

3.4 Conclusion

In conclusion, the implementation of the Matlab program ANPA is shown in what design steps are taken in order to assist the practicing engineer through the design of a pushover analysis. The resulting internal forces, reactions, and displacements are recorded at the end of each hinge formation and presented in an output document created within the ANPA file location. Displacement capacity of the structure can subsequently be checked against the spectral displacement

demand. Moment capacity checks due to the spectral acceleration and P-Delta checks can then be performed to ensure that the structure meets the requirements laid out in AASHTO. Although ANPA is not currently coded to account for geometric non-linearity under the iterative pushover process, it does have the capability to account for geometric non-linearity under static loading conditions. Therefore, it would not be too difficult to modify the coding to account for such an analysis.

Chapter 4

Verification

4.1 Introduction

The analytic equations of the internal forces and stress strain equilibrium are developed and validated in the previous chapters. In this chapter, these equations are used throughout the development of the plastic moments and hinge formations from ANPA The resulting plastic moments and hinge formations were then compared to previously validated sources. Sources implemented for this comparison include pushover and moment curvature assignments given in Professor Saouma's Nonlinear Analysis Class, results taken from SAP2000 moment curvature development software, and results taken from RISA's 3D analysis software.

4.2 Spectral Analysis Verification

To ensure that the elastic seismic coefficient is being properly calculated, the location of the Goethals Bridge is chosen to perform a spectral analysis. The USGS website has a tool that will determine acceleration coefficients for the design response spectra given certain longitudes and latitudes. By assuming a site soil classification "D", and using the initial geographic inputs provided through USGS maps, the spectral analysis can be performed in ANPA in which resulting spectral acceleration coefficients can be compared. From USGS Maps, the acceleration for the Goethals bridge are obtained in Table 4.1.

By entering these values into ANPA, the following Fig. 4.1 is obtained.

PGA	$.098g$
S_S	$.180g$
S_1	$.037g$

Table 4.1: USGS Values for Goethals Bridge

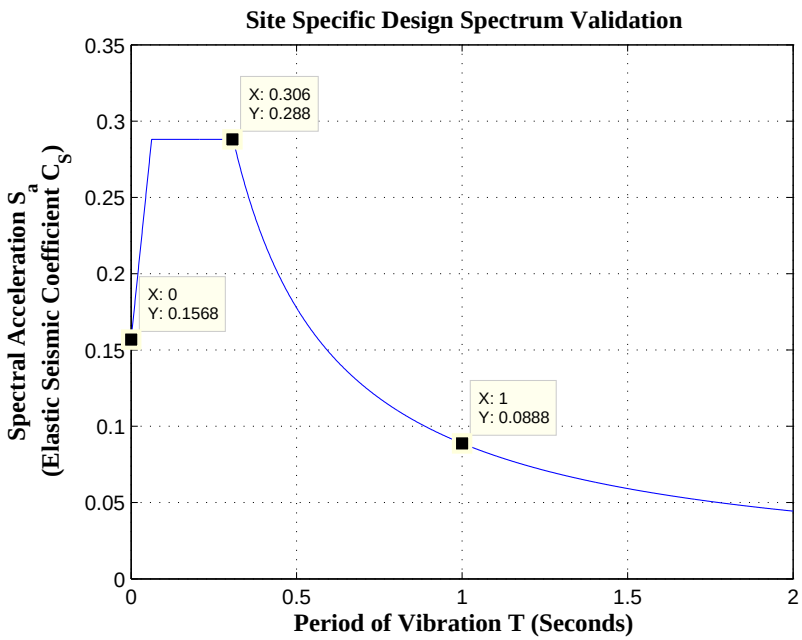

Figure 4.1: Rectangular Interaction Diagram Design Aid

From this figure, the site-specific peak ground acceleration A_s, the site-specific short-period acceleration S_{DS}, and the site specific one-second period acceleration S_{D1} are found in reading the graph from left to right. In comparison among the results obtain from USGS in Fig. 4.2, the two sets of matching data confirm that calculations used by ANPA are being carried out correctly.

USGS Design Maps Summary Report

User–Specified Input

Building Code Reference Document	2009 AASHTO Guide Specifications for LRFD Seismic Bridge Design (which utilizes USGS hazard data available in 2002)
Site Coordinates	40.63574°N, 74.19704°W
Site Soil Classification	Site Class D – "Stiff Soil"

USGS–Provided Output

PGA =	0.098 g	**A_s =**	0.156 g
S_S =	0.180 g	**S_{DS} =**	0.288 g
S_1 =	0.037 g	**S_{D1} =**	0.089 g

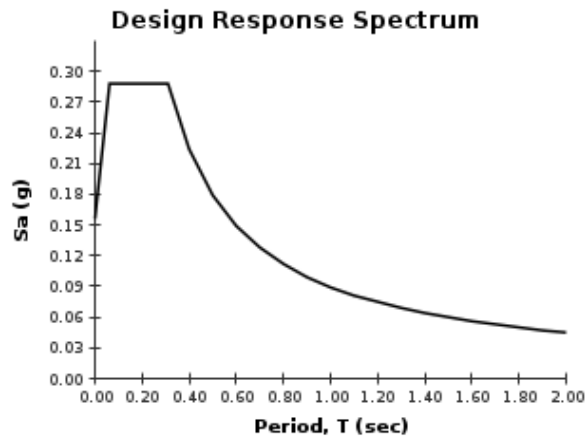

Figure 4.2: USGS Data Print out of Seismic Accelerations at Goethals Bridge

From here the Spectral Displacement can be found through the use of Eq. 2.2.

4.3 Rectangular Cross Section Interaction Diagram Validation

This section is presented to check the formation of rectangular interaction diagrams against standardized non-dimensional design aids presented by Wight, J. K. and MacGregor, J. G. (2009). The design aid is used specifically for a rectangular cross section 4 Ksi concrete and 60 Ksi steel longitudinal reinforcement in two faces as denoted in Fig. 4.3.

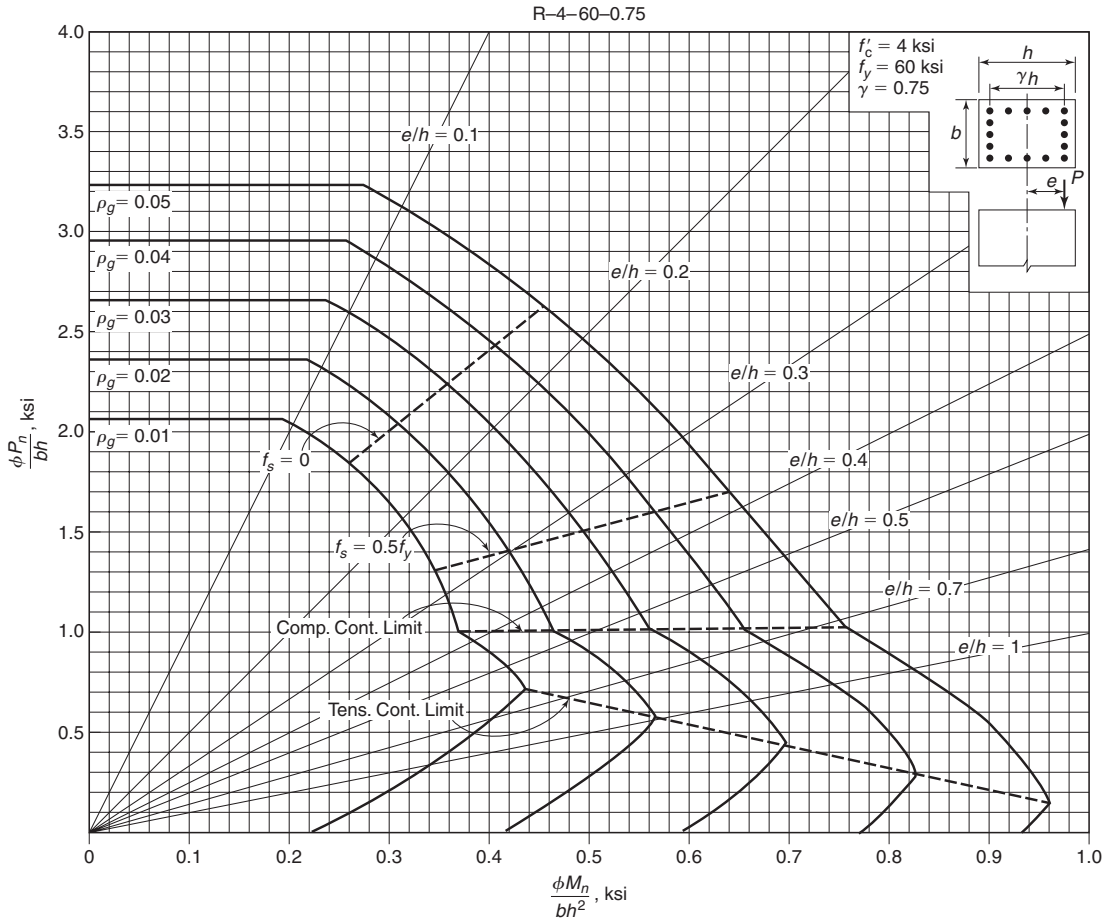

Figure 4.3: Rectangular Interaction Diagram Design Aid

Two cross sections were used to ensure that ANPA will properly model the interaction diagram for varying cross sections. The first cross section used will be a 16"x16" 4 Ksi column with 12 each #8 longitudinal 60 Ksi bars that account for ρ_g of .049. Under these conditions, the modeled interaction diagram produced should match the outermost interaction curve in Fig. 4.3. The second cross section will consist of the same outer dimensions and material properties, only with a lesser amount of reinforcement accounting for 1% of the gross area of the cross section. The resulting interaction diagram should match with the inner most curve in Fig. 4.3. Both cross sections are pictured in Fig. 4.4 with the resulting interaction curves pictured in Fig. 4.5.

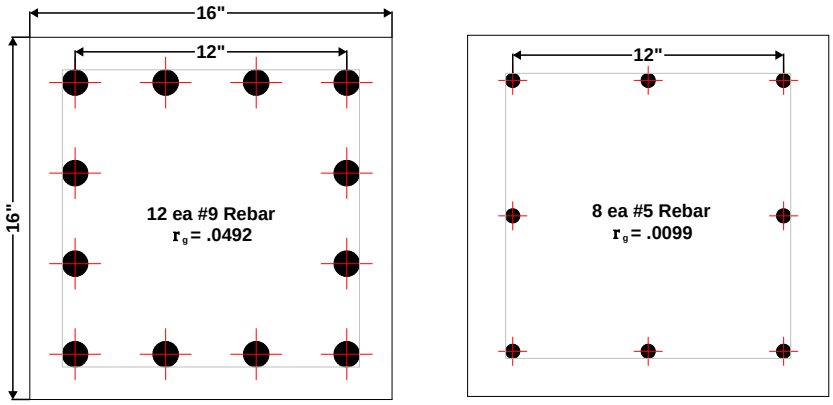

Figure 4.4: Rectangular Verification Section

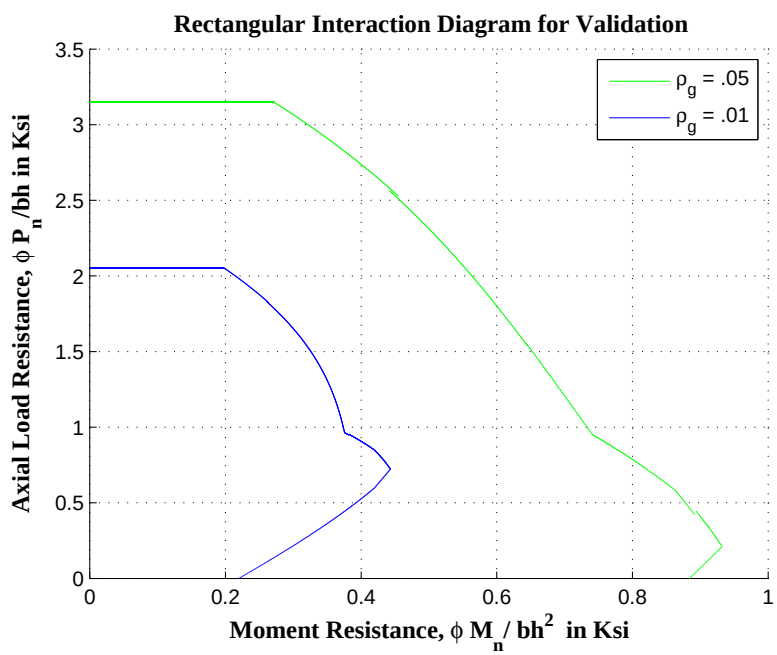

Figure 4.5: Rectangular Interaction Verification Results from ANPA

In comparison of Fig. 4.5 and 4.3, it is clear that the resulting interaction diagrams of rectangular columns produced by ANPA are being calculated correctly.

4.4 Circular Cross Section Interaction Diagram Verification

Similar to the Rectangular Cross Section Verification, this section is presented to check the formation of circular interaction diagrams against standardized non-dimensional design aids presented by Wight, J. K. and MacGregor, J. G. (2009). The design aid is used specifically for a circular cross section for 4 Ksi concrete and 60 Ksi longitudinal reinforcement as denoted in Fig. 4.3.

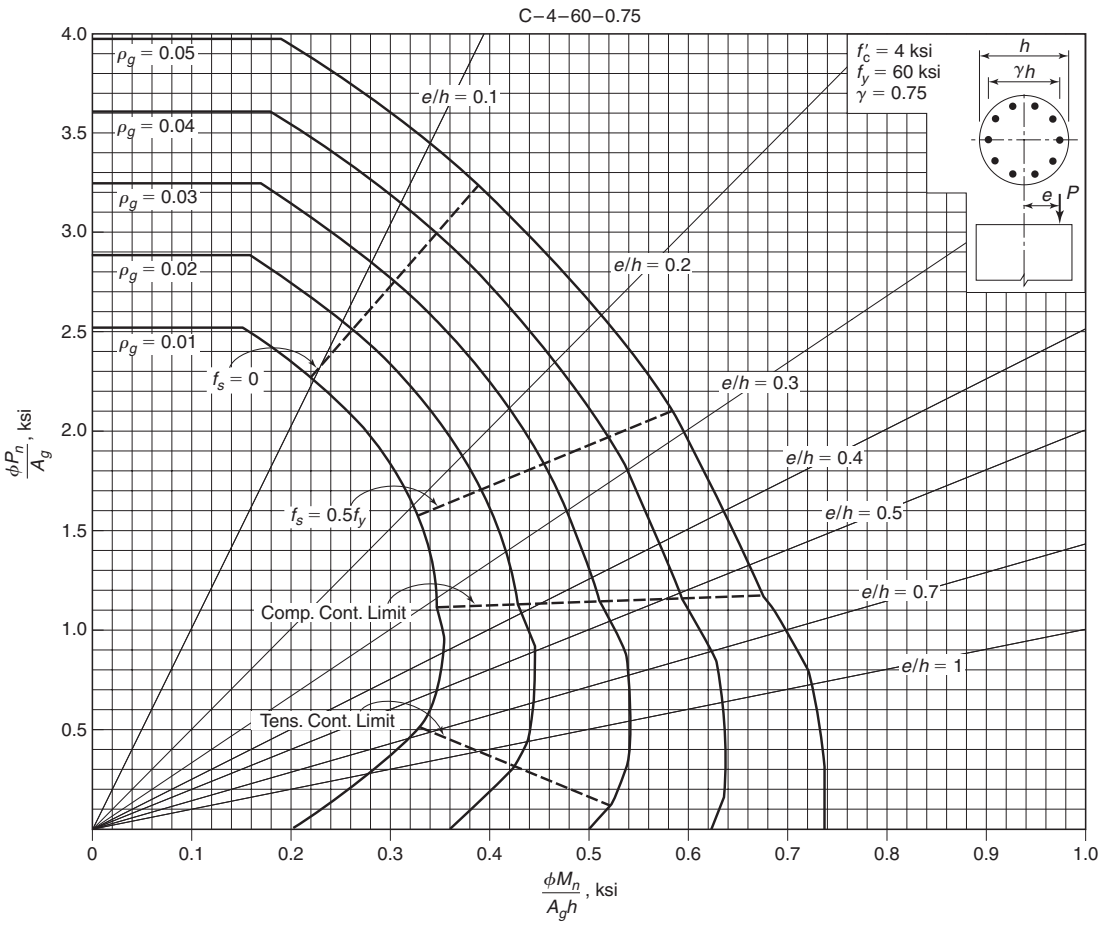

Figure 4.6: Circular Interaction Diagram Design Aid

Two cross sections were used to ensure that ANPA will properly model the interaction diagram for varying cross sections. The first cross section used will be a 16” diameter 4 Ksi column

with 10 each #8 longitudinal 60 Ksi bars that account for ρ_g of .0497. Under these conditions, the modeled interaction diagram produced should match the outermost interaction curve in Fig. 4.6. The second cross section will consist of the same outer dimensions and material properties, only with a lesser amount of reinforcement accounting for 1% of the gross area of the cross section. The resulting interaction diagram should match with the inner most curve in Fig. 4.6. Both cross sections are pictured in Fig. 4.7 with the resulting interaction curves pictured in Fig. 4.8.

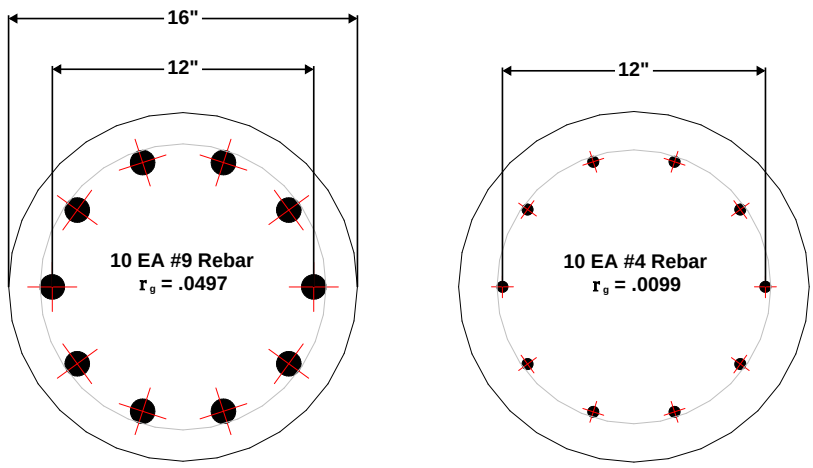

Figure 4.7: Circular Verification Selection

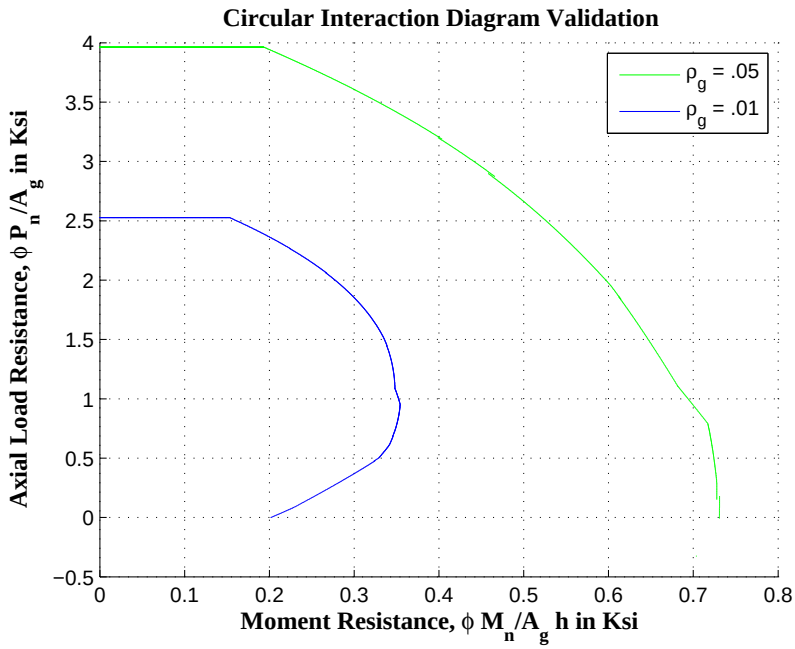

Figure 4.8: Circular Interaction Verification Results from ANPA

In comparison of Fig. 4.8 and 4.6, it is clear that the resulting interaction diagrams of circular columns produced by ANPA are being calculated correctly.

4.5 Moment Curvature & Plastic Moment Verification

This section is presented to check that the moment curvature of the concrete cross section is being calculated properly in accordance with the Mander Model for confined concrete. SAP2000's section designer program was used for the verification of ANPA. For this section two rectangular and two circular cross sections are presented and are analyzed using SAP2000 and ANPA. These cross sections and reinforcement layout are pictured in Fig. 4.9. The analysis was performed considering an unconfined concrete strength of 4 Ksi and steel strength of 60 Ksi. It is the goal of this section to show that the resulting plastic moments obtained from ANPA are within an admissible error range of ±7%. The results from both programs are depicted in Fig. 4.10.

In comparing the resulting plastic moment values, it can be said that the analyses for circular cross sections with one layer of confining reinforcement are well within the 7% limit. It should be

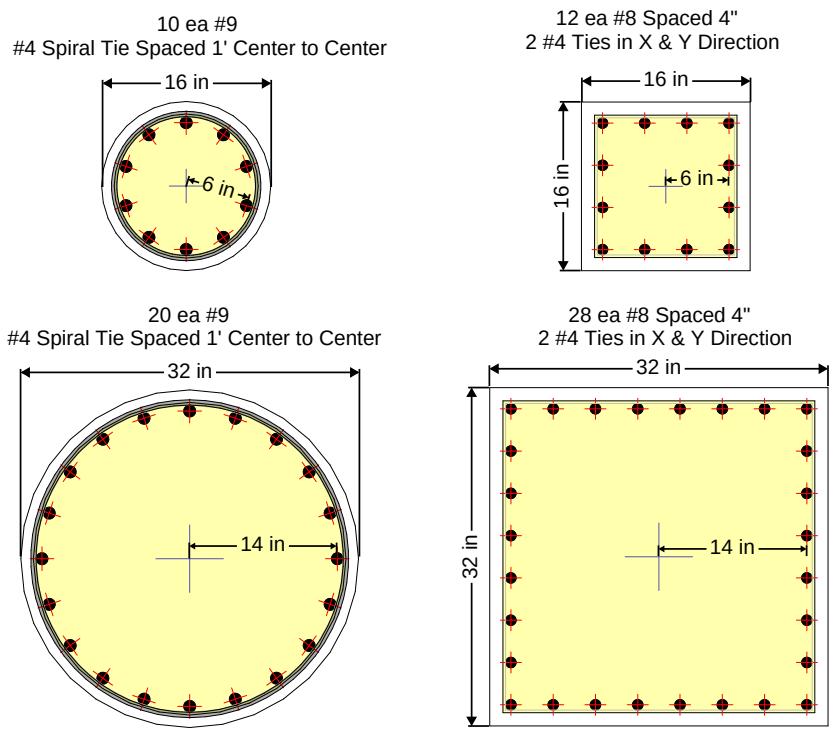

Figure 4.9: Sample Cross Sections to be Analyzed

16" Dia. Column Plastic Moment			
Axial Load (Kips)	*ANPA (K-ft)*	*SAP2000 (K-ft)*	% Error
0	236	230	2.61%
100	251	250	0.40%
200	268	264	1.52%
300	269	271	-0.74%
400	258	268	-3.73%
500	247	254	-2.76%

16"x16" Column Plastic Moment			
Axial Load (Kips)	*ANPA (K-ft)*	*SAP2000 (K-ft)*	% Error
0	217	277	-21.66%
100	248	292	-15.07%
200	265	303	-12.54%
300	267	322	-17.08%
400	274	340	-19.41%
500	276	325	-15.08%

32" Dia. Column Plastic Moment			
Axial Load (Kips)	*ANPA (K-ft)*	*SAP2000 (K-ft)*	% Error
0	1147	1131	1.41%
100	1205	1196	0.75%
200	1265	1259	0.48%
300	1323	1318	0.38%
400	1373	1369	0.29%
500	1418	1418	0.00%
1000	1567	1595	-1.76%

32"x32" Column Plastic Moment			
Axial Load (Kips)	*ANPA (K-ft)*	*SAP2000 (K-ft)*	% Error
0	1437	1517	-5.27%
100	1515	1581	-4.17%
200	1589	1656	-4.05%
300	1651	1729	-4.51%
400	1711	1805	-5.21%
500	1771	1865	-5.04%
1000	1991	2150	-7.40%

Figure 4.10: SAP to ANPA Result Comparison

noted that the area of concrete core with a radius d_s is analyzed within ANPA as the confined concrete boundary outlined by the center-line of the transverse reinforcement rather than the area of effectively confined concrete halfway between hoops or spirals. While this may lead to an overestimate of the strength of the column, ANPA ignores the strength of the unconfined concrete throughout the analysis, counter-balancing the over-strength of the confined concrete area. When comparing the results for the rectangular cross section, it can be said that the results obtained from ANPA will consistently be more conservative. Similarly to the circular cross section, SAP defines the confined area of the concrete as the area enclosed by the center-line of the transverse reinforcement. Conversely, ANPA defines the confined area of concrete as the cross-sectional area half-way between transverse reinforcement. This, in combination with the fact that ANPA ignores the strength of the unconfined concrete, produces results for smaller cross sections to be much more erroneous than for larger cross sections.

4.6 Hinge Formation Verification

This section checks to make sure that modified stiffness and geometric matrices are properly re-defined so that internal forces and displacements within a structure accurately reflect the presence of the hinge. As discussed earlier in Chapter 2, the formation of a hinge results in a zero on the axis of the stiffness matrix. In order to obtain displacements and subsequent reactions, the stiffness matrices need to be condensed so that the matrix can be properly inverted. From this process, displacements, reactions, and internal forces can be found respectively. For this analysis a fix-fix 2 dimensional bar with a hinge a third of the way across the member is analyzed with a 10 kip load at the location of the hinge. The results from ANPA are compared against the results obtained from RISA 3D. The problem statement is given in Fig. 4.11. Find the moment at each fixed end of the structure incurred by the applied load. The deformed shape of the member is denoted by the dotted outline.

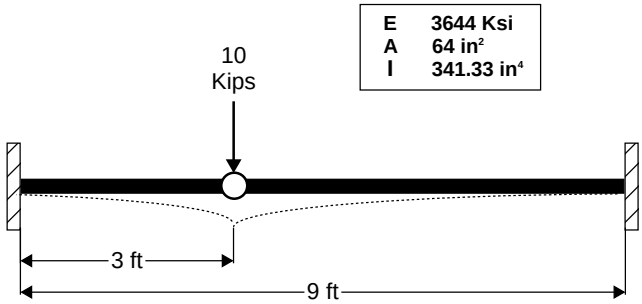

Figure 4.11: Hinge Problem Statement

The properties of the structure are based off of a normal-weight square concrete member, measured at 8" x 8" and a compression strength of 4 Ksi. These input parameters were placed into RISA and the following results were obtained.

Node	x(ft)	Shear (k)	Moment (k-ft)
1	0	8.88	26.64
2	3	–	0
3	9	−1.12	6.71

Table 4.2: RISA Fix-Fix Beam Results

The results from ANPA were obtained and are provided below

Node	x(ft)	Shear (k)	Moment (k-ft)
1	0	8.888	26.66
2	3	–	0
3	9	−1.111	6.67

Table 4.3: MPF Fix-Fix Beam Results

In comparing tables 4.2 and 4.3, it is evident that the moments obtained from ANPA and RISA are equivalent to each other. The ANPA input file and result from both programs are located in Appendix C.

4.7 Pushover Analysis Verification

This section focuses on the hinge formation sequence within a 2-d framed structure. The results obtained from the analysis will be verified with Professor Saouma's Pushover assignment. The assignment defines member properties and plastic moments that do not vary with a fluctuation in axial load on the member. By restraining the plastic moments of the members to a single variable, we simplify the design check so that only the pushover section of ANPA is under investigation.

4.7.1 Problem Statement and Expected Results

The problem statement is given in Fig. 4.12.

The upper bound theorem, or kinematic theorem, uses displacement-controlled nonlinear static analyses to solve for the exact solution, while the lower bound theorem, or static theorem, uses step-by-step load increment procedure as described earlier in Chap. 2 The stages described show at what order the hinges form before final collapse. The answer key provided in Fig. 4.13 is an exact solution, developed through the upper bound analysis. The moment at each node within the member at which cause a hinge to form is provided to further validate that the reaction, displacements, and internal forces are being calculated correctly.

In the interest of performing a static analysis to validate against, the upper bound analysis will be disregarded. To obtain results that are accurate to the nearest 100th, the incremental load is set to .01 kips. Plastic moments given were placed in the Master Excel File and the framed structure was descritized into the pushover Input File. The analysis was performed, and results were obtained in the pushover.out file. It should be noted that the answer key lists the nodes and elements starting from the left to right, following the path of the elements. The structure was descritized in such a way that the results will be organized in the same fashion the answer key is. The full print-out of this analysis is located in Appendix C.

1. Determine the collapse load for the following frame using a lower bound and an upper bound approach.

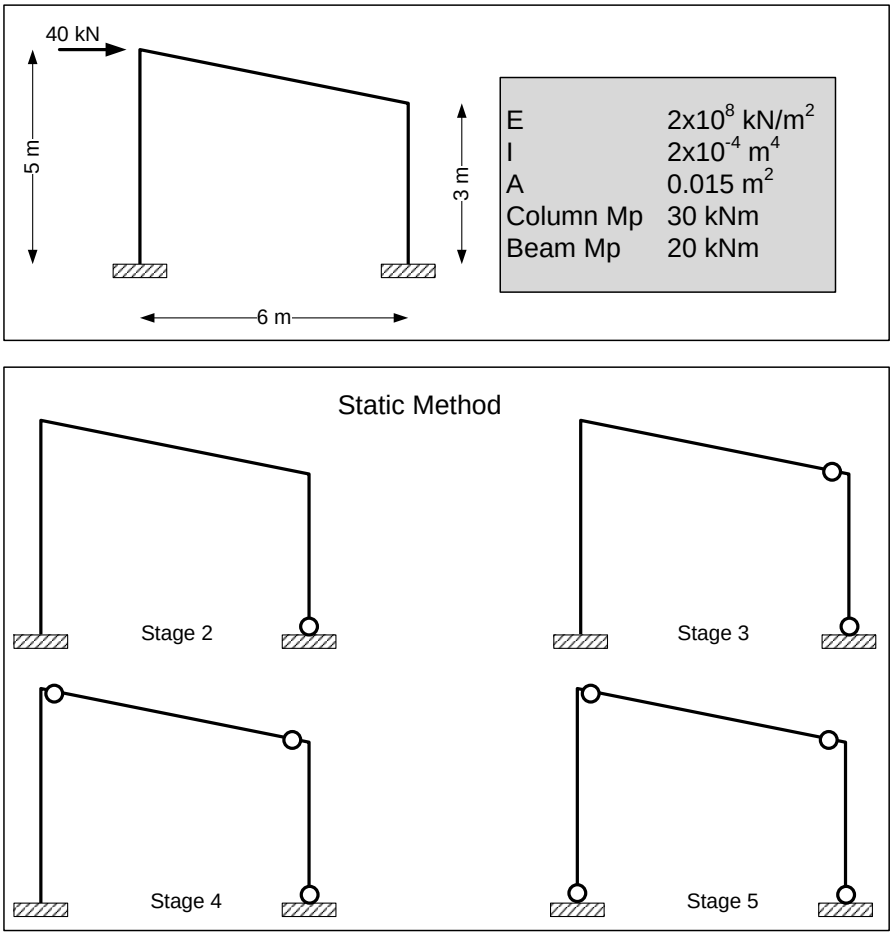

Figure 4.12: Pushover Problem Statement

Member	Joint	Moment M_0 (kNm)	Moment M_i (kNm)	Residual Plastic Moment M_p-M_i (kNm)	Load Factor $\alpha=(M_p-M_i)/M_0$	Critical Load Factor α_{cr}	Cumulative Load Factor α_{cum}	Cumulative Moment $M_{j+1}=M_j+\alpha_{cr}M_0=\alpha_{cum}M_0$ (kNm)	Plastic Moment M_p (kNm)	Critical Load $P_{cr}=P*\alpha_{cr}$ (kN)
Stage 1										
1	1	27.21	0.00	30.00	1.10	0.50	0.50	13.69	30	20.13
	2	-21.75	0.00	-30.00	1.38			-10.94	-30	
2	2	-21.75	0.00	-20.00	0.92			-10.94	-20	
	3	31.00	0.00	20.00	0.65			15.60	20	
3	3	-31.00	0.00	-30.00	0.97			-15.60	-30	
	4	59.62	0.00	30.00	0.50			30.00	30	
Stage 2										
1	1	65.09	13.69	16.31	0.25	0.08	0.59	19.14	30	23.47
	2	-47.24	-10.94	-19.06	0.40			-14.90	-30	
2	2	-47.24	-10.94	-9.06	0.19			-14.90	-20	
	3	52.61	15.60	4.40	0.08			20.00	20	
3	3	-52.61	-15.60	-14.40	0.27			-20.00	-30	
	4	0.00	0.00	0.00	0.00			0.00	30	
Stage 3										
1	1	129.70	19.14	10.86	0.08	0.07	0.66	28.55	30	26.38
	2	-70.31	-14.90	-15.10	0.21			-20.00	-30	
2	2	-70.31	-14.90	-5.10	0.07			-20.00	-20	
	3	0.00	0.00	0.00	0.00			0.00	20	
3	3	0.00	0.00	0.00	0.00			0.00	-30	
	4	0.00	0.00	0.00	0.00			0.00	30	
Stage 4										
1	1	200.00	28.55	1.45	0.01	0.01	0.67	30.00	30	26.67
	2	0.00	0.00	0.00	0.00			0.00	-30	
2	2	0.00	0.00	0.00	0.00			0.00	-20	
	3	0.00	0.00	0.00	0.00			0.00	20	
3	3	0.00	0.00	0.00	0.00			0.00	-30	
	4	0.00	0.00	0.00	0.00			0.00	30	

Figure 4.13: Pushover Answer Key

4.7.2 ANPA Results & Comparison

The results from ANPA are presented in Fig. 4.14

Hinge Formation	Element	Nodes	Moment (KN-m)	Appplied Load (KN)
Stage 1	1	1	13.69	20.13
		2	-10.94	
	2	2	-10.94	
		3	15.60	
	3	3	-15.60	
		4	30.00	
Stage 2	1	1	19.14	23.48
		2	-14.90	
	2	2	-14.90	
		3	20.00	
	3	3	-20.00	
		4	30.00	
Stage 3	1	1	28.58	26.39
		2	-20.00	
	2	2	-20.00	
		3	20.00	
	3	3	-20.00	
		4	30.00	
Faliure	1	1	30.00	26.68
		2	-20.00	
	2	2	-20.00	
		3	20.00	
	3	3	-20.00	
		4	30.00	

Figure 4.14: Pushover Results from ANPA

As we can see, the individual moments at each stage in the hinge formation process correlate to that described in the answer key. The structure reaches collapse at the applied load described in the answer key, therefore, validating that the Pushover function within ANPA is working properly no matter how the structure is descritized within the input file.

4.8 Conclusion

In conclusion, the analytic methodologies described in prior chapters are developed and verified. Every step within the pushover analysis is taken and verified against pre-existing solutions and software currently used throughout the practicing design world. The resulting interaction diagrams, plastic moments, and hinge formations are found through ANPA are found to be accurate in comparison with the sources implemented.

Chapter 5

Application

5.1 Introduction

The formulation of the conceptual model described in Chapter 2 has been formatted into a computer model and verified. This chapter aims to implement the entirety of the computer model to perform a Pushover analysis that is commonly preformed in practice. An assignment procured by Kiewit Engineering Co. for Professor Saouma's Non-Linear Structural Analysis Class will be analyzed Lefebvre, M. (2014). The assignment was to review to concepts to gain a feel for typical analyses that take place within a design firm. This report takes the assignment one step further by creating a computer program to perform the analysis. Over the course of the past year, ANPA has been created to fulfill the need of a program that can encompass the entirety of the Pushover design. The focus of the comparison will center around the plastic moments and hinge formations.

5.2 Problem Statement Provided by Kiewit

The Goethals Bridge is located outside of New York City. The main span of the bridge is a cable-stayed bridge while the two approaches are precast segmented box girders. The new bridge is replacing a steel cantilever bridge that was built in the 1920's. In this exercise, the pier design of the approach span on the New Jersey side will be analyzed given the design earthquake load. The natural period and design response spectra are given, from which the displacement demand of 6 inches is found. The structure is set up so that a 2-dimensional frame is to be analyzed. It is assumed that the cap beam is rigid, and thus, the only members needed to be taken into account

are the columns. Moreover, the shafts' connections to the bedrock are assumed to be fixed. The typical pier design is shown in Fig. 5.1

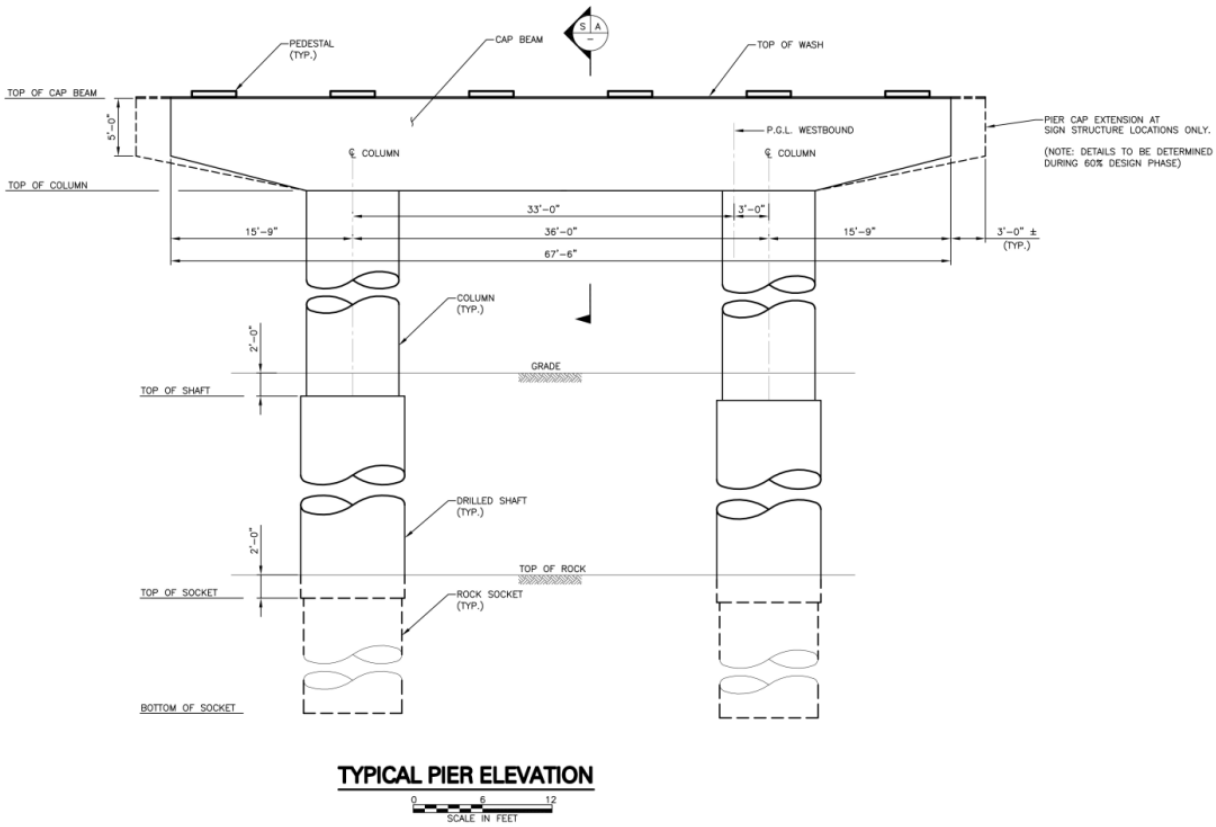

Figure 5.1: Given Pier Elevation View

From Fig. 5.1 the length of the cap beam is taken to be 36' from center to center of the supporting columns. The heights of the piers are given as a length of 100' per pier. Each pier is split into two elements with three different cross sections. The base of the pier is an 8' diameter drilled shaft that extends 60' up from the bedrock. The adjoining element is a 7' diameter column that extends the remaining 40' to the top of the cap beam. An illustration of the model denoting the elements and subsequent nodes is shown in Fig. 5.2.

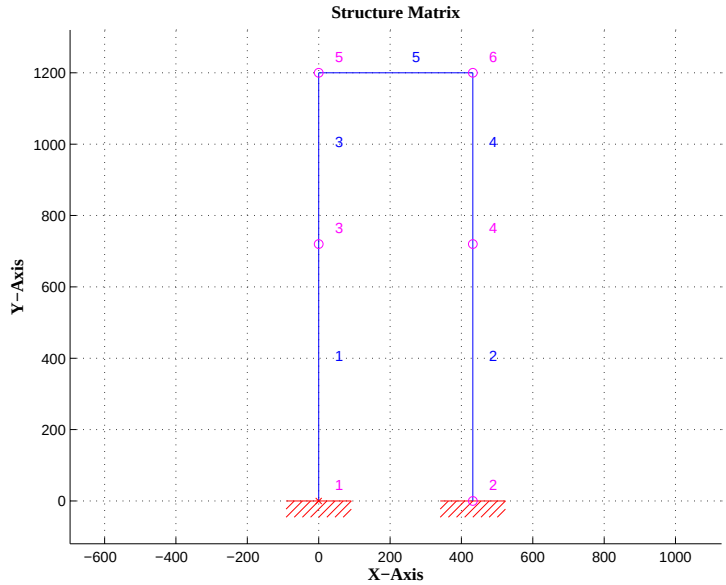

Figure 5.2: Modeled Pier Elevation View

A PDF of the structure will be produced after each hinge formation. Nodes that are assigned as hinges will appear with an "X" throughout the structure, while nodes that are still rigid will appear as a circle. As described in previous chapters, each node will hold two cross section properties belonging to the adjoining elements. The tops of element 3 and 4 are assigned the "Top 7' cross section" as shown in Fig. 5.3. This cross section is made of 5 Ksi concrete and 60 Ksi steel reinforcement. The clear cover the column was given as 2" with a transverse spacing of 6".

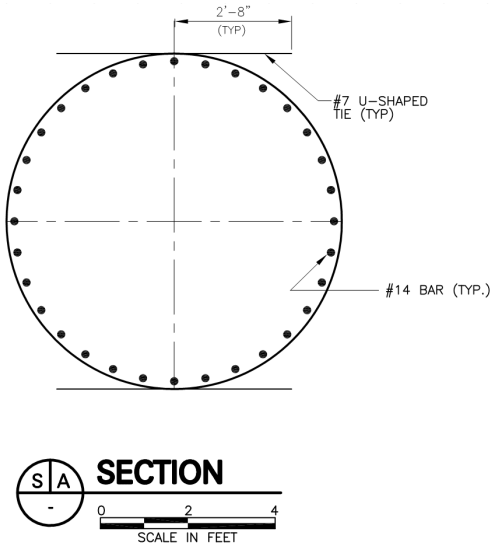

Figure 5.3: Top of 7' section

The bottom of elements 3 and 4 are assigned the "Bottom 7' section" as shown in Fig. 5.4. The column is made of 5 Ksi concrete with 60 Ksi steel. The outer layer of transverse reinforcement is discontinuous, therefore, it is to be neglected. From what was observed in the verification of the plastic moment in Section 4.5, it is expected that the results from ANPA will be more conservative than that obtained from SAP200, as there is a much smaller area of confined concrete relative to the overall size of the cross section.

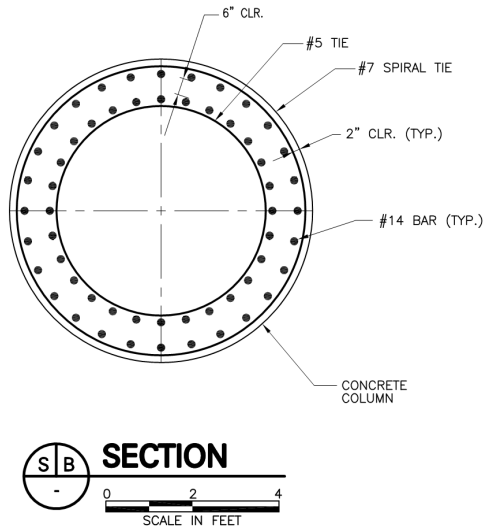

Figure 5.4: Bottom of 7' Section

The top and bottom of elements 1 and 2 are then assigned the drilled shaft cross section as shown in Fig. 5.5. The shaft is made of 4 Ksi concrete with 60 Ksi reinforcement. The section is to be analyzed neglecting the steel casing shown within the figure. The analysis of a doubly reinforced concrete section was considered outside the scope of this report and as such is recommended for future work. Both ANPA and SAP2000 only considered the outermost layer of longitudinal reinforcement during the Plastic Moment Analysis. Therefore, it is expected that the plastic moment values provided by Kiewit will be greater than that obtained through the programs previously mentioned.

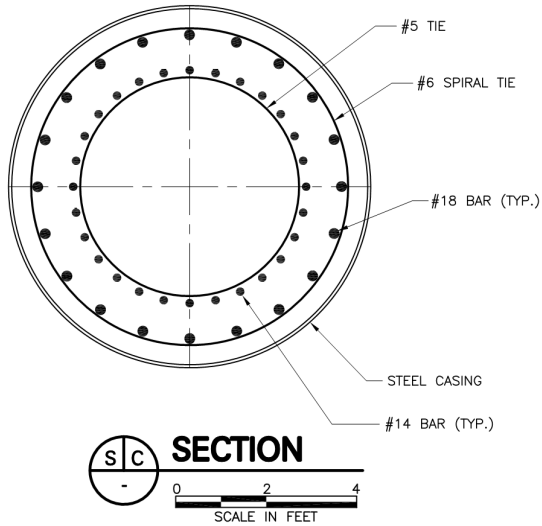

Figure 5.5: Drilled Shaft Section

A comparison of the plastic moment capacity of each cross section placed under a 2,500 Kip axial load will be preformed, followed by the hinge formation analysis containing the plastic moments obtained first from Kiewit and secondly through ANPA.

5.3 Results from ANPA & Kiewit

5.3.1 Plastic Moment Results

The Kiewit provided values, for the moment capacity of the cross-section defined in the previous section under a 2,500 Kip axial load, are defined in Fig. 5.6. Plastic Moment analyses were performed to obtain the following results From ANPA SAP2000 was then implemented to verify the results. Since it is not known where the values provided by Kiewit were obtained, accuracies of the results are based on a 7% error margin above or below the results obtained from SAP2000.

ANPA Verification			
Comparison to Kiewit's Initial Parameters			
Description	7' Dia Top (k-ft)	Comments	Within 7% error?
Kiewit	15,840		NO
ANPA	17,960	Does not take into account the strength of the unconfined concrete	YES
SAP2000	19,040	Takes into account entire cross section	
Description	7' Dia Bot (k-ft)	Comments	Within 7% error?
Kiewit	8,660		NO
ANPA	12,400	Does not take into account the strength of the unconfined concrete	
SAP2000	14,100	Takes into account entire cross section	
Description	8' Dia shaft (k-ft)	Comments	Within 7% error?
Kiewit	21,790	Takes into account that the 2nd layer of reinforcement that add to the moment capacity	YES
ANPA	19,950	Takes into account one layer of reinforcement and does not take into account the strength of the unconfined concrete	
SAP2000	21,040	Takes into account one layer of reinforcement Takes into account entire cross section	

Figure 5.6: Plastic Moment Comparisons

A quick interpretation of the results shown in Fig. 5.6 consistently show that the values obtained from Kiewit are more conservative than that obtained through ANPA which are more conservative than that obtained through SAP2000 The only outlier in the data set is the doubly reinforced shaft, to which both ANPA and SAP2000 underestimate the moment capacity as a result of just taking into account a single layer of longitudinal reinforcement. A peculiar result which leads to the most error within the data set is how far-off Kiewit's moment capacity for the cross section at the bottom of the column. As expected, the moment result from ANPA is greater than 7% lower than that obtained by SAP2000 as a consequence of SAP accounting for the added moment capacity of the unconfined concrete. However, Keiwit's moment capacity for this cross section is greater than than 40% lower in comparison to SAP2000 resulting moment capacity. Not knowing how this value was developed, it can only be advised that the Kiewit defined moment capacity for the type of a

cross section with the material properties and geometry provided is a gross underestimate of the moment capacity, found through ANPA and SAP2000, that more accurately portray the response of the actual structure.

5.3.2 Hinge Formation Results

Knowing that the moment capacities are going to be greater than the values provided by Keiwit, Two plastic Hinge Formation Analyses are performed and compared to result provided. It should be expected that the structure should have an increased incremental load capacity when utilizing the higher ANPA moment capacities. For the same reasons, it should also be expected that the structure will form hinges in locations that differ from the hinge formation order provided by Kiewit. The results from these analyses can be found below in Fig. 5.7.

Hinge Formation Results						
ANPA Hinge Analysis	ANPA M_p	*Hinge Count*	*Node at which Hinge forms*	*Moment (Kip-ft)*	*Applied Load (Kips)*	*Comments*
		1	*1*	*18,430*	*662*	Incremental load = 1 Kip
		2	*2*	*21,370*	*726*	
		3	*5*	*15,780*	*1,066*	
		4	*6*	*19,310*	*1,089*	
	Kiewit M_p	*Hinge Count*	*Node at which Hinge forms*	*Moment (Kip-ft)*	*Applied Load (Kips)*	*Comments*
		1	*5*	*13,960*	*630*	Incremental load = 10 Kips
		2	*1*	*19,390*	*710*	
		3	*6*	*17,140*	*720*	
		4	*2*	*23,510*	*740*	
Provided Values	Kiewit M_p	*Hinge Count*	*Node at which Hinge forms*	*Moment (Kip-ft)*	*Applied Load (Kips)*	*Comments*
		1	*5*	*14,190*	*670*	Incremental load = 10 Kips
		2	*1*	*19,600*	*680*	
		3	*6*	*16,040*	*720*	
		4	*2*	*22,170*	*720*	

Figure 5.7: Hinge Formation Comparison

In interpreting the results shown, the applied force is indeed higher for the analysis run with the higher moment capacities obtained through ANPA Notice, that the formation of hinges in this analysis first starts near the base of the structure and moves toward the top of the structure, where as the analysis with moment capacities provided by Kiewit follows the same hinge formation initially

provided. Notice that there are small differences in the applied loads between the hinge formation analysis using Kiewit provided plastic moments and the hinge formation result provided by Kiewit This can be attributed to the accuracy and differences of the geometric model used in developing the Kiewit results compared to the results found through ANPA. Assuming that the exact geometric measurements of the cap beam and columns are not an even 36 and 100' respectively, it can be safely assumed that the relatively small error lies within the differing geometry between the model described in the problem statement, and the model that Kiewit used to develop the provided solution guide. To fully reconcile this difference, the model Kiewit used would need to be compared against the ANPA model.

5.4 Conclusion

In conclusion, the computer model developed to perform a Pushover Analysis that is commonly preformed in practice falls is an accurate tool that can be used in the design of reinforced concrete structure. The assignment procured by Kiewit Engineering Co. for Professor Saouma's Non-Linear Structural Analysis Class denotes values that underestimate the displacement capacity of the structure, while the assignment with the implementation of ANPA procures results that are less conservative, yet still below the threshold of values defined by SAP2000. While most of the results are confined to a reasonable amount of error, it is advised that moment capacity of the cross section located at the bottom of the column be re-examined, as this was the only numerical value that was relatively smaller by a large margin.

Chapter 6

Summary

6.1 Introduction

The aim of this report was to review the theory behind the Pushover analyses of reinforced concrete structures in accordance with AASHTO Bridge Design Guidelines. A conceptual model containing the theory behind the analysis was discussed. A computer model was built to perform the analysis from beginning to finish, and print out the graphic and numerical results. Although ANPA has been developed in order to aid the design process, it is up to the practicing engineer to properly understand how the program works, and subsequently understand the input parameter and resulting numerical values.

6.2 Conclusion

In previous chapters, the design considerations and procedures are discussed in depth. Chapter 2 focuses on the theory that supports the analysis and procedure in which a pushover analysis is to be carried out. A section is dedicated to each step of the analysis, including determining the demand displacements of a structure, the plastic properties of the members within the structure, and the different pushover methods used to define the ultimate displacement capacity of the structure of interest. Chapter 3 includes the application to the means and methods of the pushover design through implementation of "ANPA". Flowcharts are provided to guide the practicing engineer though the performance of the spectral analysis the moment curvature analysis and finally the structural analysis through implementation of the direct stiffness method. Chapter 4 includes

the verification of the principle functions within ANPA. Results from the design aid are compared to proven methods and computations currently used within the field of study. The Extent of the drift at the point of collapse is considered to the the ultimate drift capacity of the structure, and is often conservative compared to the same type of analysis carried out by hand calculation.

6.3 Future Work

This report work can be further developed by expanding the current capabilities of ANPA. As described in Section 2.6.4, hinge locations can be defined to be a distance half the length of the corresponding plastic hinge length away from the node, creating another relatively small element within the structure. This would produce more realistic results in the event of the design earthquake. Another limiting assumption within ANPA is that it is not currently capable of performing a pushover analysis that includes geometric non-linearity. While the procedure does account for the material non-linearity to an extent, the model could be vastly improved if a time history analysis was added to the direct stiffness analysis within ANPA. The Study of these factors would be a valuable addition to this thesis work.

Bibliography

(2011). Building Code Requirements for Structural Concrete (ACI 318-11) and Commentary.

(2014). AASHTO Guide Specifications for LRFD Seismic Bridge Design, 2nd edition edition.

Elwi, A.A. and Murry, D.W. A 3d hypoelastic concrete constitutive relationship. Journal of Engineering Mechanics.

Lefebvre, M. (2014). Homework #10: Pushover analysis of pier. Technical report, Kiewit Engineering Co.

Mander, J. B. and Priestley, M. J. N. and Park, R. (1988). Theoretical stress-strain model for confined concrete. Journal of Structural Engineering, 114(8):1804–1825.

Olivia, M. and Mandal, P. (2005). Curvature ductility of reinforced concrete beam. Jurnal Teknik Sipil, 6(1):1–13.

Park, R. and Paulay T. (1975). Reinforced Concrete Structures. John Wiley & Sons, New-York.

Priestley, M.J.N. and Seible, F. and Calvi, G.M. (1996). Seismic Design and Retrofit of Bridges. John Wiley & Sons, Inc, 605 Third Avenue, New York 10158.

Wight, J. K. and MacGregor, J. G. (2009). Reinforced Concrete Mechanics and Design. Pearson Prentice Hall, Upper Saddle River, New Jersey 07458.

Willam, K. J. & Warnker (1975). Constitutive models for the triaxial behavior of concrete. IABSE Proceeding, 19:1–13.

Appendix A

User Manual

A.1 Introduction

This chapter aims to review how the MatLab program is set up and what its capabilities extend to. ANPA is set up with multiple functions particular to each step within the Pushover analysis. Typically interactive user input is required by a MatLab program to help guide the user through the design steps. However, this often leads to data entry mistakes and leaves the user with a vague understanding of what the program is trying to accomplish. In the interest of providing a comprehensive design tool, ANPA has been set up so that all the initial data is required prior to running the analysis. The design checks and calculation of the demand loads cannot be obtained without first defining the plastic moment of the cross section being analyzed. Therefore, the design processes that can be streamlined given the initial data provided have been lumped into ANPA. The results from this program will be printed out on a Pushover.out text file which can then be used in combination with good engineering judgment in defining the input parameters for the design check.

The design processes streamlined by ANPA consist of the following:

(1) Spectral Analysis

(2) Moment Curvature Analysis & Plastic Moment Definition

(3) Pushover Analysis (without P-Delta Effects)

The checks required after ANPA has run consist of:

(1) Check shear required for first plastic hinge to form.

(2) Check the total displacement at the top of the structure.

(3) Check if P-Delta effects need to be included.

(4) Check demand moment against the allowable moment.

A.2 Program Input

Input data for the Spectral Analysis and Moment Curvature Analysis are split up between different sheets within the Master Input File.xlsx (MIF). The input data for the pushover analysis needs to be entered into the Pushover.inp text file by a user with a decent understanding of matrix structural analysis. Let us define the input data in the order that the program will run in starting with the Master Input File. Each Excel sheet comes with a set of instructions highlighted in light yellow that define what steps need to be taken in order for the program to process properly. Cells that require user input are highlighted in bark blue with white bold lettering. All other cells that are meant to be left alone are highlighted in green.

A.2.1 Spectral Analysis Input

The first excel sheet that should be populated is the sheet labeled "Spectral Analysis Input". As mentioned in Section 2.2, the Soil Classification of the site and natural period of the structure will govern the Design Response Spectrum. These main two values that need to be defined by the project Geotechnical Eng. and Structural Eng. prior to performing the analysis.

The site acceleration values and units of displacement can be defined based on site location and user preference, respectively. In the instructions' box, there is a hyperlink that will open up the USGS maps pertaining to AASHTO Bridge Design acceleration coefficients required for the analysis. If the site classification is rated as an "F", the Geotechnical Engineer will have to provide

a site-specific Design Spectrum where the acceleration and displacement of the structure need to be determined outside of this design aid. The Spectral Analysis and Displacement pertaining to our structure can then be entered under the "Pre-Defined Values for Site Class F" section within the excel sheet. If the site class is not Class F, leave these two values as zero. Input values as they appear in the spreadsheet are displayed in Fig. A.1.

Input values from USGS maps	
Soil Class	E
	5

Geographic Values	
PGA =	**0.1**
S_S =	**0.18**
S_1 =	**0.039**

Natural Period of Structure (sec)	
Tn =	**6**

Pre-defined Values for Site Class F	
S_A	**0**
S_D	**0**

Figure A.1: Spectral Analysis Input

A.2.2 Moment Curvature

Currently ANPA is set up to analyze four types of cross sections that need to be defined as such:

(1) Circular Cross Section defined as Type 1

(2) Rectangular Cross Section defined as Type 2

(3) Steel Cross section defined as Type 3

(4) User defined Mp defined as Type 4

Cross sections will vary throughout a structure depending the loading demand that certain parts of a structure will be required to meet. For this purpose, the program allows for three different sections to be defined per type of cross section. This information needs to be entered into ANPA under the Plastic Moment section of the program. For example, if a concrete column as a particular reinforcement layout at the top of the column and a different reinforcement layout at the bottom of the column, the information would need to be placed as follows:

$Type = [1, 1]$

The connectivity between the cross sections and their location within the elements of the structure can then be defined.

A.2.2.1 Input For A Circular Cross Section

Each cross section will be defined in the sheets' Circular Confined Input 1, 2, and 3 respectively. Currently, the program can is set up to analyze a cross section with a single layer of reinforcement with up to 36 longitudinal bars per layer. If only one RC section is defined in ANPA, the input for Circular Confined Input 2 and 3 can be ignored. Likewise, if only two cross sections are defined in ANPA, the 3rd input worksheet can be ignored. The excel sheets are consistent in that the radius and spacing measurements of the reinforcement are always measured to the center of the bar for both longitudinal and transverse reinforcement. Fig. A.2 highlight what values need to be entered in by the user. The next value to be defined is the type of transverse reinforcement, which can be defined as either Hooped or Spiral Reinforcement and is denoted as either a 1 or a 2 by the program. Material properties for both concrete and steel can then be defined. Steel can be chosen between Grade 60 A706 or A615 for the analysis. While these two materials perform the same under elastic deformations, the A706 has a higher ultimate tensile strain which we will need later when the program calculates the ultimate strain of the structure. The last section to fill out contains the maximum axial load to be analyzed, the axial load increments, and the strain

Column Dimensions		
Descrip.	Units	(r_c)
Radius	in	42

Reinforcement Dimensions					
Descrip.	Units	Outermost Longitudinal Rein. (r_1)	Outermost Transverse Rein. (r_{s1})	Inner Longitudinal Rein. (r_2)	Inner Transverse rein. (r_{s2})
Radius	in	38.279	39.5625	0.000	0
Qty	ea	28	-	0	-
Spacing	in	-	4.5	-	0
Size (#)	#	14	7	0	0
Bar Dia.	in	1.693	0.875	-	0.000
Bar Area	in^2	2.250	0.600	-	0.000
Alpha/Bar	rad	0.224	-	-	-
Spiral/Hoop Tie	Spiral = 1 Hoop = 2	-	2	-	0

Iteration Precision			Material Properties		
Axial Load Increments			Concrete Composition		
P delta =	2500	kips	f'_c	5	Ksi
Strain Parameters			Steel Composition		
Delta Strain	0.0005	in/in	A706 = 1; A615 = 2		1
Max Axial Load					
P max =	2500	kips			

Figure A.2: Circular Cross Section Input

increments that we want our analysis to take into account. These three values have a relatively large effect on the processing time required to run the analysis. A point on the moment curvature diagram will be plotted for each strain increment. An increment between .0001 and .0005 is a small enough value to produce a well-defined moment curvature plot that can be used to accurately define the nominal moment of the section under a given axial load. A visual comparison between a strain of .0001 and .0005 is given in Fig. for the 7' column at the top of the pier under nil axial load.

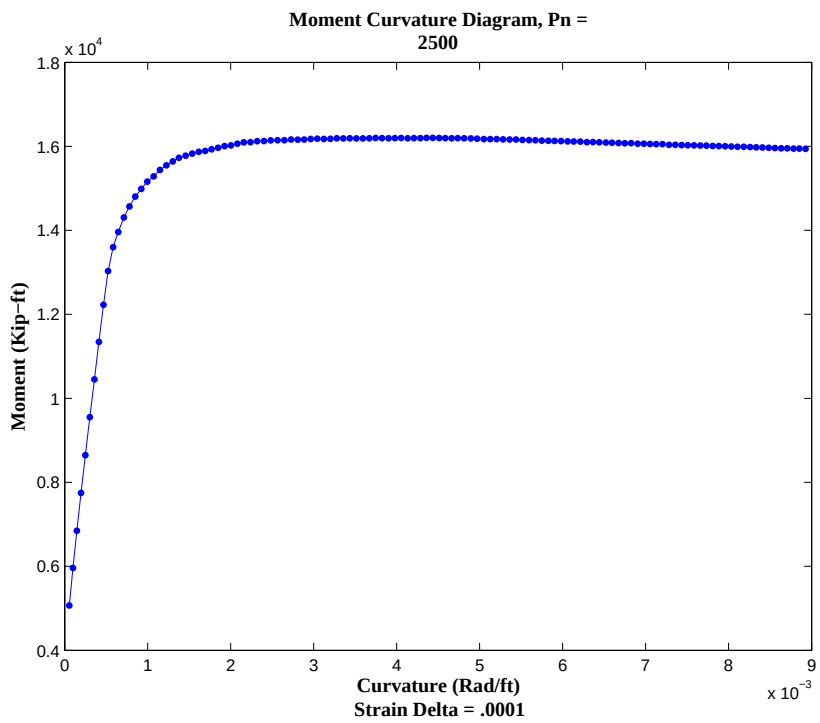

Figure A.3: Moment Curvature Diagrams with .0001 Strain Increments

It is estimated to take approximately 5 times longer to obtain the moment-curvature plot when utilizing a .0001 strain increment in comparison to a .0005 strain increment. The accuracy gained by performing an analysis with the smaller strain increment is summarized in Table A.1.

As we can see there is little value to increasing the strain increment. In order to obtain the plastic moment of a section over a range of axial loads, this graphing process needs to be performed for every axial load increment. Once all the variables are filled out within "Confined Circular Input

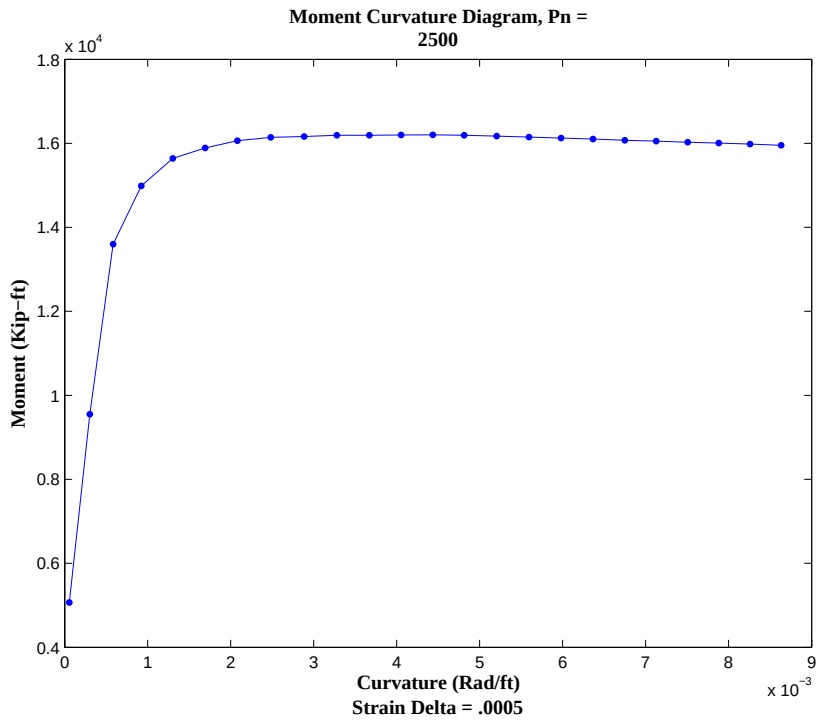

Figure A.4: Moment Curvature Diagrams with .0005 Strain Increments

$\varepsilon = .0001$	$10,562K - ft$
$\varepsilon = .0005$	$10,608K - ft$
Percent Error:	.4%

Table A.1: Error Analysis

1, 2, & 3", open up the worksheet "Circular d Values 1, 2, & 3". This worksheet brings in the longitudinal reinforcement areas and dimensions and groups bars at the same dimension d into singular variables. An example of this is displayed in Fig. A.5 below

Separate Bars		Combined	
Area in^2	"d"	Area in^2	"d"
2.25	3.722	2.25	3.722
2.25	4.681	4.5	4.681
2.25	4.681	0	0.000
2.25	7.512	4.5	7.512
2.25	7.512	0	0.000

Figure A.5: Rebar Dimension Grouping

A.2.2.2 Input for A Steel Cross Section

In chapter 4, we will perform a pushover analysis on a steel structure in order to check that the pushover program is functioning properly. To simplify the analysis, we will account for the formation of a plastic hinge once the applied moment reaches the plastic moment of the section, regardless of the axial forces imposed on the member in combination with the applied moment. By defining the member and grade of steel, the Master Input File will populate the plastic moment from the electronically stored AISC manual in the last worksheet of the excel file. Similar to the circular RC cross section, up to three steel cross sections can be defined within the analysis. Axial load increments and max axial loads for this section do not affect the processing time of the analysis, but still need to be defined in order for the program to function correctly. Strain increments do not need to be defined as we can calculate the plastic moment provided the Z_x value given by AISC. Fig. A.6 defines what values should be defined.

A.2.2.3 User Defined Input

If the plastic moments corresponding axial loads are already known, the values can be entered in the worksheet labeled "$UserDefinedMp$". ANPA will recognize up to 50 plastic moment values

Member Details						
Cross Section #	AISC Manual Label	F_y (KSI)	Z_x (in^3)	Mp (kip-ft)	Axial Load Increment (kips)	Max Axial Load (kips)
1	W44X335	60	1620	8100	100	2500
2	W44X335	60	1620	8100	100	2500
3	W44X335	60	1620	8100	100	2500

Figure A.6: Steel Cross Section Input

per cross section. This sheet works in much the same way as the others as the blue fields require user input accompanied by an instructional table highlighted in yellow. The axial load and up to three cross sections can be filled out in the excel sheet. A summary of what can be filled out is given in Fig. A.7

Member Details				
Axial Load P (K)	Cross Section # and Mp (K-ft)			
	1	2	3	Rigid
0	10858	5051	16234	1E+10
100	11067	5216	16467	1E+10
200	11276	5379	16698	1E+10

Figure A.7: User Defined Cross Section Input

If we choose to have a rigid member in our structure, assign a relatively large plastic moment to the member to ensure that the plastic moments of the rigid will not be reached during analysis. As an example, we will use a moment of $1^{10}K - ft$ for the rigid member in our validation efforts in Chap. 4

A.2.3 Pushover Input

The Pushover analysis requires the use of a "computer-assisted structural analysis software", or CASAP that is regularly used by Professor Saouma's Advanced Structural Analysis class. For this project, CASAP was modified to recognize the formation of hinges and subsequently re-order the stiffness and geometric matrices. The input for this program is labeled as Pushover.inp and can be found in the folder labeled CASAP This file should be opened with MatLab as it is not

formatted to easily be read within Notepad or other text reading software. The file is set up to analyze a 2-d framed structure. It is essential that the structure be idealized such that it can be discretized down to a node/element level within the structure. As noted previously, the user is required to have a firm understand of matrix structural analysis in order to correctly define the initial input data.

A.2.3.1 Input Parameter Descriptions

The input parameters are listed and defined as follows:

`npoin` This variable defines the number of nodes within the structure. A node can be defined as a point where two or more elements within a structure connect.

`nelem` This variable defines the number oif elements within a structure. An element can be defined as the physical member that spans between nodes.

`nload` This variable defines the number of load cases imposed on the structure. Because we will only be increasing the load at a particular node, we can set this value equal to 1.

`_ID` This matrix contains the boundary conditions imposed on each node. the number of rows within the matrix correspond to the number of nodes within the structure. The matrix is three columns wide to correspond with the three degrees of freedom for each node within the 2-D frame. Constrained degrees of are denoted with a value of 1, while free degrees of freedom should be denoted by a value of 0.

`nodecoor` This matrix contains the coordinates of the nodes in the global coordinate system. The matrix is 2 columns wide to correspond with the x and y axis, and the number of rows correspond to the number of nodes within the structure.

`lnods` This is the element connectivity matrix where each row corresponds to the element number within the structure, and the columns correspond with the node numbers at which the element is connected from and to.

`Mp_xsec` This is the plastic moment connectivity matrix where the rows of the matrix correspond to the cross section location within the structure, and the columns correspond to the range of plastic moment values per cross section. There is a cross section denoted at each end of an element and as such, the rows are ordered by the node numbers at which the element is connected from and to.

`hingeperc` This is the design value at which we can expect a hinge to form within the structure.

Phi This is the hinge matrix that will be populated with zeros once hinges start forming throughout the analysis. Rather than having a hinge form within an element a certain distance away from a node, this matrix will place a pin at the node at which the hinge forms next to.

`unit` This variable defines what units the analysis should be performed in.

`Pdel` This Variable defines whether or not the analysis should include P-Delta Effects. This program has not been modified to accurately predict P-Delta effects after the formation of the first hinge formation, therefore, it is advised that this program not be used if P-Delta effects need to be taken into account.

`E, A, Iz` These arrays are the material and cross-sectional properties for the elements. They are arrays with the number of terms equal to the number of elements within the structure. E is the modulus of elasticity of the member. A is the cross-sectional area of the member, and Iz is the moment of inertia.

`IncFreeDOF` This is the global degree of freedom within the structure that we want to increase our load on during the pushover analysis. The Program will only accept a single degree of freedom in which the pushover load can be applied.

`IncVal` This is the incremental value in which the pushover load is increased.

`Pnods` This is the array of constant nodal loads in global degrees of freedom. The index number within the array corresponds with the number of global degrees of freedom. Therefore, a

zero should be placed within the array for each GDOF that does not have a load.

`Pelem` This is an array of element point loads that which are applied on elements in local coordinates. The index number corresponds with the element number. If there isn't a point load on the physical member, place a zero in the appropriate index value. The program is not currently set up to handle this type of load, therefore, place zeros for every value.

`a` This is an array that defines where the point loads defined in Pelem are located. The index number corresponds to the number of elements in the structure. The value of each number denotes the distance the node is located from the left end of the element. The program is not currently set up to handle this type of load, therefore, place zeros for every value.

`w` This is an array of distributed loads of elements within the structure in local coordinates. The Index number corresponds with the element number. If there is not a load on the member, place a zero for the index value. The program is not currently set up to handle this type of load, therefore, place zeros for every value.

A.2.4 Program Results

To run the program, open up ANPA and click "run". The program will run the pushover analysis until the stiffness matrix becomes unstable. Stability within the structure can be defined by the formation of a mechanism, or more simply put, the ability for any part of the structure to freely rotate under it's own weight. At this point, ANPA will halt the pushover analysis and will return a file labeled *Pushover.out* which can be read as a text file in Notepad. Among the data returned are the spectral acceleration and displacement from the Spectral Analysis, the axial loads and corresponding plastic moments from the Moment Curvature Analysis, and data structures resulting from each subsequent hinge formation.

Appendix B

Pushover Input Listings

XXXXXX

B.1 Main Program

```
function [Geom,Prop,Force] = input_file(Mp)
%*****************************************************************************************
%   Scriptfile name:    Pushover.inp     (EXAMPLE 2D FRAME INPUT DATA)
%
%   Main Program:   casap.m
%
%       This is the main data input file for the computer aided
%       structural analysis program CASAP.  The user must supply3.09
%       the required numeric values for the variables found in
%       this file (see user's manual for instructions).
%
%   Variable descriptions:  (in the order in which they appear)
%
%       npoin        =    number of nodes in the structure
%       nelem        =    number of elements in the structure
%       nload        =    number of different load cases to be analyzed
%       orig_ID      =    information concerning the boundary conditions
%       nodecoord    =    global coordinates of the nodes in the structure
%       lnods        =    nodal connectivity information.
%       Mp_xsec      =    cross section connectivity information.
%       hingeperc    =    percent of plastic moment at which hinge forms
%       Phi          =    hinge connectivity information.
%       unit         =    units in which the analysis is to be run
%       Pdel         =    toggle P Delta effects
%       E(ielem)     =    modulus of elasticity of element ielem
%       A(ielem)     =    cross sectional area of element ielem
%       Iz(ielem)    =    moment of inertia with respect to the local z axis of element ielem
%       IncFreeDOF   =
%       IncVal       =
%       Pnods        =    array of nodal loads in global degrees of freedom
%       Pelem        =    element loads or loads which are applied between nodes
```

```
%       a           =    distance from the left end of an element to the element load
%       w           =    distributed loads on the structure
%
%*****************************************************************************************
%% Structure type
istrtp = 3;
%% This is a set of dummy values for this variables needed for 3D analysis
G = 0;Ix = 0;Iy = 0;
%   SET NPOIN EQUAL TO THE NUMBER OF NODES IN THE STRUCTURE
npoin = 6;
%   SET NELEM EQUAL TO THE NUMBER OF ELEMENTS IN THE STRUCTURE
nelem = 5;
%   SET NLOAD EQUAL TO THE NUMBER OF LOAD CASES
nload = 1;
%   INPUT THE ID MATRIX CONTAINING THE NODAL BOUNDARY CONDITIONS (ROW #  =
%   NODE #)
orig_ID = [1,1,1;
       1,1,1;
       0,0,0;
       0,0,0;
       0,0,0;
       0,0,0];

%   INPUT THE NODE COORDINATE (X,Y) MATRIX, NODECOOR (ROW #  =  NODE #)
%   STRUCTURAL PROPERTIES UNITS: ft(m)
nodecoor = [
    0,0;
    36,0;
    0,60;
    36,60;
    0,103.5;
    36,103.5];

%   INPUT THE ELEMENT CONNECTIVITY MATRIX, LNODS (ROW #  =  ELEMENT #)
lnods= [1,3;
        2,4;
        3,5;
        4,6;
        5,6];

%   ASSIGN THE PLASTIC MOMENT CROSS SECTION TO EACH ELEMENT IN INCREMENTAL ORDER EX:
%[elem1(i);elem1(j);elem2(i); etc.]

Mp_xsec = [Mp(3,:);
           Mp(3,:);
           Mp(3,:);
           Mp(3,:);
           Mp(2,:);
           Mp(1,:);
           Mp(2,:);
           Mp(1,:);
```

```
            Mp(4,:);
            Mp(4,:)];

%   Hinge forms at   % of Mp

hingeperc = .95;

%   INPUT THE ELEMENT HINGE MATRIX (1 RIDGED, 0 HINGE)
Phi = [1,1;
        1,1;
        1,1;
        1,1;
        1,1];

%   CHOOSE BETWEEN SI(1) OR METRIC(2) UNITS
unit = 1;

%   CHOOSE TO INCLUDE GEOMETRIC NON LINEARITY (P DELTA) (1) OR NOT (2)
Pdel = 2;

%   INPUT THE MATERIAL PROPERTIES AND CROSS SECTIONAL CHARACTERISTICS ASSOCIATED WITH THIS
%   TYPE OF STRUCTURE PUT INTO ARRAYS WHERE THE INDEX NUMBER IS EQUAL TO THE CORRESPONDING
%   ELEMENT NUMBER.
%   STRUCTURAL PROPERTIES UNITS: kip/in^2(kN/m^2), in^2(m^2), in^4(m^4)
%   NOTE: 1 GPA = 1*10^6 KN/M^2
E   =  [3605*[1 1],4031*[1 1], 10^10];
A   =  [7238.23*[1,1],5541.77*[1,1, 1] ];
Iz  =  [4169220*[1,1],2443920*[1,1,1] ];
%   INPUT THE LOAD DATA.
%       PNODS: NODAL LOADS. IF THERE ARE NO NODAL LOADS, PNODS SHOULD BE EQUAL TO 'NONE', OTHERWISE
%   PNODS SHOULD BE IN MATRIX FORM: THE COLUMNS CORRESPOND TO THE GLOBAL DEGREE OF FREEDOM
%   IN WHICH THE LOAD IS ACTING AND THE THE ROW NUMBER CORRESPONDS WITH THE LOAD CASE NUMBER.
%       PELEM: ELEMENT LOAD IN Y DIRECTION (LOCAL COORDINATE SYSTEM WITH ELEMENT AXIS IN X DIRECTION),
%   GIVEN IN A MATRIX, WITH COLUMNS CORRESPONDING TO THE ELEMENT NUMBER AND ROW THE LOAD CASE.
%       A: DISTANCE FROM THE LEFT END OF THE ELEMENT TO THE LOAD, IN ARRAY FORM (LOCAL COORDINATE
%   SYSTEM).
%       W: DISTRIBUTED LOAD IN Y DIRECTION, SHOULD BE IN MATRIX FORM WITH COLUMNS = ELEMENT
%   NUMBER UPON WHICH W IS ACTING AND ROWS = LOAD CASE.
%       ZEROS SHOULD BE USED IN THE MATRICES WHEN THERE IS NO LOAD PRESENT.  NODAL LOADS SHOULD
%   BE GIVEN IN GLOBAL COORDINATES, WHEREAS THE ELEMENT LOADS AND DISTRIBUTED LOADS SHOULD BE
%   GIVEN IN LOCAL COORDINATES.
%   LOAD UNITS: Position in Pnods, Kip(Kn), Kip(Kn), Kip(Kn), ft(m), Kip/ft(Kn/m)
IncFreeDOF = 7;
IncVal = 1;
Pnods = [0;0;0;  0;0;0; 0; 2500;0; 0; 2500;0];
Pelem = [0,0,0,0,0];
a = [0,0,0,0,0];
w = [0,0,0,0,0];
%% Assign to structure Data
Geom.istrtp = istrtp;
Geom.npoin = npoin;
```

```
Geom.nelem = nelem;
Geom.orig_ID = orig_ID;
Geom.unit = unit;
Geom.Phi = Phi;
Geom.lnods = lnods;
Geom.hingeperc = hingeperc;
Prop.E = E;
Prop.G = G;
Prop.A = A;
Prop.Ix = Ix;
Prop.Iy = Iy;
Prop.Iz = Iz;
Prop.Pdel = Pdel;
Prop.Mp_xsec = Mp_xsec;
Force.nload = nload;
Force.Pnods = Pnods;
Force.Pelem = Pelem;
Force.IncPnod = IncFreeDOF;
Force.IncVal = IncVal;

%CONVERT LENGTH OF ELEMENTS INTO INCHES
if unit == 1
    Geom.nodecoor = nodecoor.*12
    Force.a = a.*12;
    Force.w = w.*12;
else
    Geom.nodecoor = nodecoor;
    Force.a = a;
    Force.w = w;
end
end
%%    End Script
```

Appendix C

Pushover Verification Listings

C.1 Steel Frame Output File

```
%%                Steel 2 D Fame Pushover Analysis Check                %%
 ----------------------------------------------------------------------

BEGIN ANALYSIS WITH THE FOLLOWING NUMBER OF HINGES :  0
Apply Incremental Load of_0.01 at Unrestrained DOF# :  1
Analysis Stopped When Hinge #1 Forms at Node :  4
Total Applied Incremental Load at End of Analysis:  2.013000e+01

 ----------------------------------------------------------------------

Number of Nodes :  4
Number of Elements :  3
Number of Load Cases :  1
Hinge #1 Formed at :  4
Number of Restrained dofs :  6
Number of Free dofs :  6

Node Info :
     Node 1 (0,0)
        Free dofs :  none; node is fixed
     Node 2 (0,5)
        Free dofs :   X  Y  ROT
     Node 3 (6,3)
        Free dofs :   X  Y  ROT
     Node 4 (6,0)
        Free dofs :  none; node is fixed

Element Info :
     Element 1 (1  > 2)   E = 200000000 A = 1.500000e 02  Iz = 2.000000e 04
     Element 2 (2  > 3)   E = 200000000 A = 1.500000e 02  Iz = 2.000000e 04
     Element 3 (3  > 4)   E = 200000000 A = 1.500000e 02  Iz = 2.000000e 04

 ----------------------------------------------------------------------

```

```
Load Case :  1

   Nodal Loads :
     Node :   2 Fx =   2.013000e+01

   Elemental Loads :
     Element :  1   Point load = 0 at 0 from left
                    Distributed load = 0
     Element :  2   Point load = 0 at 0 from left
                    Distributed load = 0
     Element :  3   Point load = 0 at 0 from left
                    Distributed load = 0

   Displacements:
     (Node:  2 delta X)   1.712490e 03
     (Node:  2 delta Y)   1.582010e 05
     (Node:  2 rotate )   1.717599e 04
     (Node:  3 delta X)   1.665332e 03
     (Node:  3 delta Y)   9.492061e 06
     (Node:  3 rotate )   5.401114e 04

   Reactions:
     (Node:  1 Fx)   4.927068e+00
     (Node:  1 Fy)   9.492061e+00
     (Node:  1 M )   1.369175e+01
     (Node:  4 Fx)   1.520293e+01
     (Node:  4 Fy)   9.492061e+00
     (Node:  4 M )   3.000588e+01

   Internal Forces:
      Element:  1
       At Node: 1
          (Global : Fx )   4.927068e+00    (Local Total: Fx )   9.492061e+00
          (Global : Fy )   9.492061e+00    (Local Total: Fy )   4.927068e+00
          (Global : M  )   1.369175e+01    (Local Total: M  )   1.369175e+01
       At Node: 2
          (Global : Fx )   4.927068e+00    (Local Total: Fx )   9.492061e+00
          (Global : Fy )   9.492061e+00    (Local Total: Fy )   4.927068e+00
          (Global : M  )   1.094359e+01    (Local Total: M  )   1.094359e+01

-----------------------------------------------------------------------

   Internal Forces:
      Element:  2
       At Node: 2
          (Global : Fx )   1.520293e+01    (Local Total: Fx )   1.742442e+01
          (Global : Fy )   9.492061e+00    (Local Total: Fy )   4.197371e+00
          (Global : M  )   1.094359e+01    (Local Total: M  )   1.094359e+01
       At Node: 3
          (Global : Fx )   1.520293e+01    (Local Total: Fx )   1.742442e+01
          (Global : Fy )   9.492061e+00    (Local Total: Fy )   4.197371e+00
```

```
          (Global : M  )   1.560291e+01    (Local Total: M  )   1.560291e+01

 ----------------------------------------------------------------------

   Internal Forces:
      Element:  3
       At Node: 3
          (Global : Fx )   1.520293e+01    (Local Total: Fx )   9.492061e+00
          (Global : Fy )   9.492061e+00    (Local Total: Fy )   1.520293e+01
          (Global : M  )   1.560291e+01    (Local Total: M  )   1.560291e+01
       At Node: 4
          (Global : Fx )   1.520293e+01    (Local Total: Fx )   9.492061e+00
          (Global : Fy )   9.492061e+00    (Local Total: Fy )   1.520293e+01
          (Global : M  )   3.000588e+01    (Local Total: M  )   3.000588e+01

 ----------------------------------------------------------------------


 ----------------------------------------------------------------------
 ----------------------------------------------------------------------

BEGIN ANALYSIS WITH THE FOLLOWING NUMBER OF HINGES :  1
Apply Incremental Load of_0.01 at Unrestrained DOF# :  1
Analysis Stopped When Hinge #2 Forms at Node :  3
Total Applied Incremental Load at End of Analysis:  2.348000e+01

 ----------------------------------------------------------------------

Number of Nodes :  4
Number of Elements :  3
Number of Load Cases :  1
Hinge #1 Formed at :  4
Hinge #2 Formed at :  3
Number of Restrained dofs :  5
Number of Free dofs :  7

Node Info :
     Node 1 (0,0)
        Free dofs :  none; node is fixed
     Node 2 (0,5)
        Free dofs :   X  Y  ROT
     Node 3 (6,3)
        Free dofs :   X  Y  ROT
     Node 4 (6,0)
        Free dofs :   ROT

Element Info :
     Element 1 (1  > 2)   E = 200000000 A = 1.500000e 02  Iz = 2.000000e 04
     Element 2 (2  > 3)   E = 200000000 A = 1.500000e 02  Iz = 2.000000e 04
     Element 3 (3  > 4)   E = 200000000 A = 1.500000e 02  Iz = 2.000000e 04

```

```
---------------------------------------------------------------------

Load Case :  1

   Nodal Loads :
     Node :   2 Fx =   3.350000e+00

   Elemental Loads :
     Element :  1   Point load = 0 at 0 from left
                  Distributed load = 0
     Element :  2   Point load = 0 at 0 from left
                  Distributed load = 0
     Element :  3   Point load = 0 at 0 from left
                  Distributed load = 0

   Displacements:
     (Node:  2 delta X)   7.235745e 04
     (Node:  2 delta Y)   3.138580e 06
     (Node:  2 rotate )   9.345013e 05
     (Node:  3 delta X)   7.174812e 04
     (Node:  3 delta Y)   1.883148e 06
     (Node:  3 rotate )   1.290158e 04
     (Node:  4 rotate )             0

   Reactions:
     (Node:  1 Fx)   1.881405e+00
     (Node:  1 Fy)   1.883148e+00
     (Node:  1 M )   5.451113e+00
     (Node:  4 Fx)   1.468595e+00
     (Node:  4 Fy)   1.883148e+00

   Internal Forces:
      Element:  1
       At Node: 1
          (Global : Fx )   1.881405e+00    (Local Total: Fx )   1.137521e+01
          (Global : Fy )   1.883148e+00    (Local Total: Fy )   6.808473e+00
          (Global : M  )   5.451113e+00    (Local Total: M  )   1.914286e+01
       At Node: 2
          (Global : Fx )   1.881405e+00    (Local Total: Fx )   1.137521e+01
          (Global : Fy )   1.883148e+00    (Local Total: Fy )   6.808473e+00
          (Global : M  )   3.955911e+00    (Local Total: M  )   1.489950e+01

---------------------------------------------------------------------

   Internal Forces:
      Element:  2
       At Node: 2
          (Global : Fx )   1.468595e+00    (Local Total: Fx )   1.941316e+01
          (Global : Fy )   1.883148e+00    (Local Total: Fy )   5.519471e+00
          (Global : M  )   3.955911e+00    (Local Total: M  )   1.489950e+01
       At Node: 3
```

```
          (Global : Fx )   1.468595e+00    (Local Total: Fx )   1.941316e+01
          (Global : Fy )   1.883148e+00    (Local Total: Fy )   5.519471e+00
          (Global : M  )   4.405785e+00    (Local Total: M  )   2.000870e+01

 ----------------------------------------------------------------------

   Internal Forces:
      Element:  3
       At Node: 3
          (Global : Fx )   1.468595e+00    (Local Total: Fx )   1.137521e+01
          (Global : Fy )   1.883148e+00    (Local Total: Fy )   1.667153e+01
          (Global : M  )   4.405785e+00    (Local Total: M  )   2.000870e+01
       At Node: 4
          (Global : Fx )   1.468595e+00    (Local Total: Fx )   1.137521e+01
          (Global : Fy )   1.883148e+00    (Local Total: Fy )   1.667153e+01
          (Global : M  )              0    (Local Total: M  )   3.000588e+01

 ----------------------------------------------------------------------



 ----------------------------------------------------------------------
 ----------------------------------------------------------------------

BEGIN ANALYSIS WITH THE FOLLOWING NUMBER OF HINGES :  2
Apply Incremental Load of_0.01 at Unrestrained DOF# :  1
Analysis Stopped When Hinge #3 Forms at Node :  2
Total Applied Incremental Load at End of Analysis:  2.639000e+01

 ----------------------------------------------------------------------

Number of Nodes :  4
Number of Elements :  3
Number of Load Cases :  1
Hinge #1 Formed at :  4
Hinge #2 Formed at :  3
Hinge #3 Formed at :  2
Number of Restrained dofs :  5
Number of Free dofs :  7

Node Info :
     Node 1 (0,0)
        Free dofs :  none; node is fixed
     Node 2 (0,5)
        Free dofs :   X  Y  ROT
     Node 3 (6,3)
        Free dofs :   X  Y  ROT
     Node 4 (6,0)
        Free dofs :   ROT

Element Info :
     Element 1 (1  > 2)   E = 200000000 A = 1.500000e 02  Iz = 2.000000e 04
```

```
    Element 2 (2 > 3)   E = 200000000 A = 1.500000e 02 Iz = 2.000000e 04
    Element 3 (3 > 4)   E = 200000000 A = 1.500000e 02 Iz = 2.000000e 04

----------------------------------------------------------------------

Load Case :  1

  Nodal Loads :
    Node :   2 Fx =   2.910000e+00

  Elemental Loads :
    Element :  1   Point load = 0 at 0 from left
                 Distributed load = 0
    Element :  2   Point load = 0 at 0 from left
                 Distributed load = 0
    Element :  3   Point load = 0 at 0 from left
                 Distributed load = 0

  Displacements:
    (Node:  2 delta X)   1.432800e 03
    (Node:  2 delta Y)   1.420844e 06
    (Node:  2 rotate )   2.699951e 04
    (Node:  3 delta X)   1.431443e 03
    (Node:  3 delta Y)   8.525065e 07
    (Node:  3 rotate )             0
    (Node:  4 rotate )             0

  Reactions:
    (Node:  1 Fx)   2.910000e+00
    (Node:  1 Fy)   8.525065e 01
    (Node:  1 M )   9.434961e+00
    (Node:  4 Fx)   5.220097e 17
    (Node:  4 Fy)   8.525065e 01

  Internal Forces:
     Element:  1
      At Node: 1
         (Global : Fx )   2.910000e+00    (Local Total: Fx )   1.222772e+01
         (Global : Fy )   8.525065e 01    (Local Total: Fy )   9.718473e+00
         (Global : M  )   9.434961e+00    (Local Total: M  )   2.857782e+01
      At Node: 2
         (Global : Fx )   2.910000e+00    (Local Total: Fx )   1.222772e+01
         (Global : Fy )   8.525065e 01    (Local Total: Fy )   9.718473e+00
         (Global : M  )   5.115039e+00    (Local Total: M  )   2.001454e+01

----------------------------------------------------------------------

  Internal Forces:
     Element:  2
      At Node: 2
         (Global : Fx )   9.858780e 14    (Local Total: Fx )   1.968274e+01
```

```
          (Global : Fy )   8.525065e 01    (Local Total: Fy )   6.328230e+00
          (Global : M  )   5.115039e+00    (Local Total: M  )   2.001454e+01
       At Node: 3
          (Global : Fx )   9.858780e 14    (Local Total: Fx )   1.968274e+01
          (Global : Fy )   8.525065e 01    (Local Total: Fy )   6.328230e+00
          (Global : M  )              0    (Local Total: M  )   2.000870e+01

-----------------------------------------------------------------------

   Internal Forces:
      Element:  3
       At Node: 3
          (Global : Fx )   5.220097e 17    (Local Total: Fx )   1.222772e+01
          (Global : Fy )   8.525065e 01    (Local Total: Fy )   1.667153e+01
          (Global : M  )              0    (Local Total: M  )   2.000870e+01
       At Node: 4
          (Global : Fx )   5.220097e 17    (Local Total: Fx )   1.222772e+01
          (Global : Fy )   8.525065e 01    (Local Total: Fy )   1.667153e+01
          (Global : M  )              0    (Local Total: M  )   3.000588e+01

-----------------------------------------------------------------------



-----------------------------------------------------------------------
-----------------------------------------------------------------------

BEGIN ANALYSIS WITH THE FOLLOWING NUMBER OF HINGES :  3
Apply Incremental Load of_0.01 at Unrestrained DOF# :  1
Analysis Stopped When Hinge #4 Forms at Node :  1
Total Applied Incremental Load at End of Analysis:  2.668000e+01

-----------------------------------------------------------------------

Number of Nodes :  4
Number of Elements :  3
Number of Load Cases :  1
Hinge #1 Formed at :  4
Hinge #2 Formed at :  3
Hinge #3 Formed at :  2
Hinge #4 Formed at :  1
Number of Restrained dofs :  5
Number of Free dofs :  7

Node Info :
     Node 1 (0,0)
        Free dofs :  none; node is fixed
     Node 2 (0,5)
        Free dofs :   X  Y  ROT
     Node 3 (6,3)
        Free dofs :   X  Y  ROT
     Node 4 (6,0)
```

```
        Free dofs :   ROT

Element Info :
     Element 1 (1 > 2)   E = 200000000 A = 1.500000e 02 Iz = 2.000000e 04
     Element 2 (2 > 3)   E = 200000000 A = 1.500000e 02 Iz = 2.000000e 04
     Element 3 (3 > 4)   E = 200000000 A = 1.500000e 02 Iz = 2.000000e 04

----------------------------------------------------------------------

Load Case :  1

   Nodal Loads :
     Node :   2 Fx =   2.900000e 01

   Elemental Loads :
     Element :  1   Point load = 0 at 0 from left
                  Distributed load = 0
     Element :  2   Point load = 0 at 0 from left
                  Distributed load = 0
     Element :  3   Point load = 0 at 0 from left
                  Distributed load = 0

   Displacements:
     (Node:  2 delta X)   3.020833e 04
     (Node:  2 delta Y)   1.954108e 20
     (Node:  2 rotate )             0
     (Node:  3 delta X)   3.020833e 04
     (Node:  3 delta Y)   2.049749e 20
     (Node:  3 rotate )             0
     (Node:  4 rotate )             0

   Reactions:
     (Node:  1 Fx)   2.900000e 01
     (Node:  1 Fy)   6.440468e 16
     (Node:  1 M )   1.450000e+00
     (Node:  4 Fx)   1.224783e 31
     (Node:  4 Fy)   2.000223e 15

   Internal Forces:
      Element:  1
       At Node: 1
          (Global : Fx )   2.900000e 01    (Local Total: Fx )   1.222772e+01
          (Global : Fy )   6.440468e 16    (Local Total: Fy )   1.000847e+01
          (Global : M  )   1.450000e+00    (Local Total: M  )   3.002782e+01
       At Node: 2
          (Global : Fx )   2.900000e 01    (Local Total: Fx )   1.222772e+01
          (Global : Fy )   6.440468e 16    (Local Total: Fy )   1.000847e+01
          (Global : M  )             0    (Local Total: M  )   2.001454e+01

----------------------------------------------------------------------
```

```
   Internal Forces:
      Element:  2
       At Node: 2
          (Global : Fx )   2.550487e 14    (Local Total: Fx )   1.968274e+01
          (Global : Fy )   6.133146e 15    (Local Total: Fy )   6.328230e+00
          (Global : M  )              0    (Local Total: M  )   2.001454e+01
       At Node: 3
          (Global : Fx )   2.550487e 14    (Local Total: Fx )   1.968274e+01
          (Global : Fy )   6.133146e 15    (Local Total: Fy )   6.328230e+00
          (Global : M  )              0    (Local Total: M  )   2.000870e+01

 ----------------------------------------------------------------------

   Internal Forces:
      Element:  3
       At Node: 3
          (Global : Fx )   1.224783e 31    (Local Total: Fx )   1.222772e+01
          (Global : Fy )   2.000223e 15    (Local Total: Fy )   1.667153e+01
          (Global : M  )              0    (Local Total: M  )   2.000870e+01
       At Node: 4
          (Global : Fx )   1.224783e 31    (Local Total: Fx )   1.222772e+01
          (Global : Fy )   2.000223e 15    (Local Total: Fy )   1.667153e+01
          (Global : M  )              0    (Local Total: M  )   3.000588e+01

 ----------------------------------------------------------------------
%%    End Script
```

C.2 Hinge Formation Validation Listings

```
 ----------------------------------------------------------------------

%%           Hinge Formation Results of a Fix Fix Bar              %%

 ----------------------------------------------------------------------

Number of Nodes :  3
Number of Elements :  2
Number of Load Cases :  1
Number of Restrained dofs :  6
Number of Free dofs :  3

Node Info :
     Node 1 (0,0)
        Free dofs :  none; node is fixed
     Node 2 (3,0)
        Free dofs :   X  Y  ROT
     Node 3 (9,0)
        Free dofs :  none; node is fixed

```

```
Element Info :
     Element 1 (1 > 2)   E = 3644 A = 64 Iz = 3.413300e+02
     Element 2 (2 > 3)   E = 3644 A = 64 Iz = 3.413300e+02
   Displacements:
     (Node:  2 delta X)              0
     (Node:  2 delta Y)   6.431869e 05
     (Node:  2 rotate )              0

   Reactions:
     (Node:  1 Fx)              0
     (Node:  1 Fy)   8.888889e+00
     (Node:  1 M )   2.666667e+01
     (Node:  3 Fx)              0
     (Node:  3 Fy)   1.111111e+00
     (Node:  3 M )   6.666667e+00

   Internal Forces:
      Element:  1
       At Node: 1
          (Global : Fx )              0    (Local : Fx )              0
          (Global : Fy )              0    (Local : Fy )   8.888889e+00
          (Global : M  )              0    (Local : M  )   2.666667e+01
       At Node: 2
          (Global : Fx )              0    (Local : Fx )              0
          (Global : Fy )              0    (Local : Fy )   8.888889e+00
          (Global : M  )              0    (Local : M  )              0

      Element:  2
       At Node: 2
          (Global : Fx )              0    (Local : Fx )              0
          (Global : Fy )              0    (Local : Fy )   1.111111e+00
          (Global : M  )              0    (Local : M  )              0
       At Node: 3
          (Global : Fx )              0    (Local : Fx )              0
          (Global : Fy )              0    (Local : Fy )   1.111111e+00
          (Global : M  )              0    (Local : M  )   6.666667e+00

-----------------------------------------------------------------------
```

RISA Hinge Formation Validation

Concrete Properties

	Label	E [ksi]	G [ksi]	Nu	Therm (\1E...	Density[k/ft...	f'c[ksi]	Lambda	Flex Steel[...	Shear Stee...
3	Conc4000NW	3644	1584	.15	.6	.145	4	1	60	60

Joint Boundary Conditions

	Joint Label	X [k/in]	Y [k/in]	Z [k/in]	X Rot.[k-ft/rad]	Y Rot.[k-ft/rad]	Z Rot.[k-ft/rad]	Footing
1	N1	Reaction	Reaction	Reaction	Reaction	Reaction	Reaction	
2	N3	Reaction	Reaction	Reaction	Reaction	Reaction	Reaction	

Joint Loads and Enforced Displacements (BLC 1 : 1)

	Joint Label	L,D,M	Direction	Magnitude[(k,k-ft), (in,rad), (k*s^2/ft...
1	N2	L	Y	-10

Member Section Forces (By Combination)

	LC	Member Label	Sec	Axial[k]	y Shear[k]	z Shear[k]	Torque[k-ft]	y-y Mo...	z-z Moment[k-ft]
1	1	M1	1	0	8.88	0	0	0	26.641
2			2	0	8.88	0	0	0	19.98
3			3	0	8.88	0	0	0	13.32
4			4	0	8.88	0	0	0	6.66
5			5	0	8.88	0	0	0	0
6	1	M2	1	0	-1.12	0	0	0	0
7			2	0	-1.12	0	0	0	1.68
8			3	0	-1.12	0	0	0	3.359
9			4	0	-1.12	0	0	0	5.039
10			5	0	-1.12	0	0	0	6.719

Figure C.1: RISA Hinge Fix-Fix Bar Output file